COMPARISON OF FINITE ELEMENT AND INFLUENCE FUNCTION METHODS FOR THREE-DIMENSIONAL ELASTIC ANALYSIS OF BOILING WATER REACTOR FEEDWATER NOZZLE CRACKS

EPRI NP-261
(Research Projects 700 and 498)

Key Phase Report

November 1976

Prepared by

Failure Analysis Associates
750 Welch Road
Palo Alto, California 94304

Teledyne Materials Research
303 Bear Hill Road
Waltham, Massachusetts 02154

Authors
Philip M. Besuner
Walter R. Caughey

Prepared for

Electric Power Research Institute
3412 Hillview Avenue
Palo Alto, California 94304

Project Managers
Terry Oldberg
Floyd Gelhaus

NOTICE

This report was prepared by Failure Analysis Associates (FAA) and Teledyne Materials Research as an account of work sponsored by the Electric Power Research Institute, Inc. (EPRI). Neither EPRI, members of EPRI, FAA, Teledyne Materials Research, nor any person acting on behalf of either: (a) makes any warranty or representation, express or implied, with respect to the accuracy, completeness or usefulness of the information contained in this report, or that the use of any information, apparatus, method, or process disclosed in this report may not infringe privately owned rights; or (b) assumes any liabilities with respect to the use of, or for damages resulting from the use of, any information, apparatus, method, or process disclosed in this report.

FOREWORD

It is remarkable that the Influence Fuction Method has gone largely unused as a practical means for solving a wide variety of complex stress-analysis-of-crack problems. Under contract to the Electric Power Research Institute (EPRI), Failure Analysis Associates has developed a Three-Dimensional Influence Function (IF) Method. The 3-D IF Method is applicable to most elastic crack problems and is especially useful to account for complex stress field, geometry, and boundary condition features.

This technique is now used for solving a large class of fracture mechanics and fatigue analysis problems with known uncracked stress fields, where the crack growth problems were once treated only by Finite Element analyses. For example, stress, fracture, and fatigue analyses employing the 3-D IF technique have been applied accurately and inexpensively in problems involving cracks in:

- Nuclear power plant components (especially regions of the pressure vessels)
- Bearings
- Automobile parts
- Suspension bridge structural members
- Wind tunnels
- Railroad rails
- Piping
- Sections of broadcast towers
- Supertanker ship-welds
- Jet engine rotors and static structures.

This report shows that, for a series of crack analysis test cases with known solutions, the 3-D Influence Function Method yielded more accurate results and cost 2000 times less in direct computer charges than the state-of-the-art applied Finite Element algorithm.

Floyd Gelhaus, Project Manager, RP 700-1
Terry Oldberg, Project Manager, RP 498-1

ABSTRACT

This paper compares the finite element (FE) and influence function (IF) methods for a three-dimensional elastic analysis of postulated circular-shaped surface cracks in the feedwater nozzle of a typical boiling water reactor (BWR). The complex nature of the stress gradients and geometry of the feedwater nozzle region require that accurate numerical methods be employed to calculate stress intensity factors. The stress intensity factors are used in fracture mechanics-based fatigue and brittle failure analyses which are performed to judge whether or not a given crack-like flaw is acceptable for the remaining service life of the vessel. Currently employed nozzle flaw evaluation methods, as in Section XI of the ASME Boiler and Pressure Vessel Code, are limited to simple geometries and linear gradients of stress.

This report compares two possible methods for determining stress intensity factors for nozzle corner cracks. The FE method is incorporated in a direct manner. The nozzle and crack geometry and the complex loading are all included in the model which simulates the structural crack problem. The IF method is used to compute stress intensity factors only when the uncracked stress field (that is, the stress in the uncracked solid at the locus of the crack to be eventually considered) has been computed previously. The IF method evaluates correctly the disturbance of this uncracked stress field caused by the crack by utilizing a method of elastic superposition. Both the IF and FE methods are described in detail in the paper and are applied to several test cases chosen for their similarity to the nozzle crack problem and for the availability of an accurate published result obtained from some recognized third method of solution. Results are given which summarize both the accuracy and the direct computer costs of the two methods for each of the selected

test cases. The IF method is demonstrated to be superior from both an accuracy and cost viewpoint. The FE method, as applied to cases where the uncracked stress field has been determined previously, was more than one thousand times more costly than the IF method and had average errors of 3 to 5% as compared to 1% for the IF method. On the basis of these results, the IF method has been chosen by the Electric Power Research Institute to perform current and future evaluations of nozzle flaws in the remaining phases of this study. The FE method is shown to be of acceptable accuracy and is recommended for flaw evaluation for cases lacking certain adequate IF results. These IF results are required for utilization of the IF method and are usually available in the literature or derivable from crack opening displacement information.

TABLE OF CONTENTS

LIST OF FIGURES

LIST OF FIGURES
(Continued)

LIST OF TABLES

1.0 BACKGROUND AND INTRODUCTION

The feedwater nozzle in the boiling water reactor pressure vessel is a particularly important structural region because of relatively high stress levels, complex geometry, large stress gradients, and the in-service inspection requirements imposed by Section XI of the ASME Boiler and Pressure Vessel Code (1). This combination of difficult-to-inspect geometry, high stress levels, and resulting relatively small Code-allowable flaw sizes may lead to internal inspection of the nozzle and to the removal of unacceptable flaws by grinding. These two operations require several days of plant down-time at a cost to the power industry of $250,000 to $1,000,000 per day depending upon local replacement fuel costs (25). Furthermore, the cumbersome hand flaw evaluation analysis which has been done in the past also takes significant time and should be improved, automated, and streamlined as in (27) to increase accuracy and save time. Feedwater nozzle flaws have already been encountered and, in some cases, removed by grinding in several pressure vessels.

Of prime importance in the flaw evaluation is the calculation of stress intensity factors K under crack opening (Mode I) loads. According to an engineering discipline called fracture mechanics, K embodies the effects of stress field, crack size, shape, and location, and local structural geometry upon residual fatigue life and static strength of a cracked structural element under nominally elastic loads.

Very little guidance is available in the Code to handle the complexity of the fracture mechanics-based stress intensity factor calculations required to judge whether or not a given flaw is acceptable. The methods in Section XI, Appendix A are limited to simple

geometries and linear gradients of stress. In Appendix G of Section III, reference is made to a better, non-mandatory, methodology for nozzles contained in Welding Research Council Bulletin #175, "PVRC Recommendations on Toughness Requirements for Ferritic Materials" (10). However, the specific procedures of WRC 175, based on a specific 3-D finite element analysis by Rashid and Gilman (2), is intended solely for pressure loadings and cannot account for several important factors. Specific effects that cannot be handled adequately are thermal and cladding stress gradients, flaw locations different than considered in (2), and such three-dimensional complications as variation of K around the crack front and non-self similar fatigue crack growth.

Both the finite element (FE) and influence function (IF) methods have the potential to allow evaluation of the three-dimensional complications described above for the BWR nozzle crack problem. The FE method is well established as a numerical structural analysis tool, but at the outset of this study, it was anticipated that the FE method would be rather costly for direct three-dimensional analysis of cracks. Therefore an IF method, which has been developed specifically for practical solution of three-dimensional problems by one of the authors (3), was also evaluated because of its potential to 1) increase accuracy, 2) reduce costs, and 3) shorten the time for the nozzle crack analysis.

Section 2 outlines the influence function method as applied in this study. As explained in Section 2, a stress analysis of the uncracked structure is required; the influence function method calculates the disturbance of the uncracked stress field due to the presence of a crack. Section 3 describes the procedures used to apply a basic, three-dimensional FE analysis approach to the nozzle crack problem. As

discussed in Section 3, a strain energy release rate calculation is performed to minimize error and costs of the available finite element analysis algorithm. This applied algorithm (22) was chosen primarily on the basis of availability, familiarity, and ease of application, and it does not make use of either high-order elements nor special three-dimensional crack tip elements. Section 4 compares the accuracy and computer-time cost of the IF and FE methods for five test cases that were considered. Both error and cost of fracture mechanics analysis are shown to be significantly lower for the IF method. It is also noted that both the FE and IF results are in reasonable agreement with literature solutions, and it is concluded in Section 5 that the FE method, as applied in Section 4, may be used in the absence of usually available or derivable IF solutions to obtain adequate results for three-dimensional crack analysis.

2.0 INFLUENCE FUNCTION DERIVATIONS AND STRESS INTENSITY FACTOR COMPUTATIONS

The formulation and application of the IF method have been developed and demonstrated elsewhere (3,13) and in the first part of this section, we include a brief review only for completeness. The second part of the section presents the results of a new numerical K_I solution for a semicircular surface crack under Mode I loading and discusses other solutions utilized in this investigation.

2.1 Review of the Influence Function Method

Figure 1 illustrates the elastic superposition principle which is the basis of the IF method. For simplicity, the illustration considers a two-dimensional problem; the derivation of all three-dimensional methods used in this report may be found in (3). The superposition reduces the K solution of an arbitrary and, perhaps, difficult crack problem to the solution of 1) the problem without the crack, and 2) a crack problem in which only the crack face is loaded so as to cancel the uncracked stresses ($\sigma(x)$ in Fig. 1) that would exist across the crack locus in the absence of the crack. Influence functions are used to solve this second pressurized crack problem. An influence function h is simply the K value arising from a unit point load at some position, usually on the crack face. Thus h is independent of loading, as proven rigorously in (3 and 7) and depends only on the crack face position, displacement constraints, and structural geometry. For rigorous solution of any mixed boundary value problem, but especially to solve displacement-constrained thermal-mechanical problems, it is imperative

to model displacement constraints correctly in the IF solutions of Fig. 2.

Following Fig. 2., we solve the pressurized crack problem, and hence, the difficult original problem, by considering the differential load $\sigma(x)\,dx$ (assuming constant thickness) which causes a differential increment of K given by

$$dK(x) = h\,(x, \text{constraints, geometry})\;\sigma\,(x)\;dx \qquad (2.1)$$

so that the stress intensity factor is given by

$$K = \int_{L_a} dK(x) = \int_{L_a} h(x, \text{constraints, geometry})\sigma(x)\;dx \qquad (2.2)$$

where L_a is the straight crack face boundary parallel to the x axis.

The description above is for a general two-dimensional Mode I elastic crack problem. By analogy, and as proven rigorously in (3), the stress intensity factor solution for three-dimensional Mode I planar crack problems can be expressed by

$$\overline{K} = \iint_A h(x, y, \text{constraints, geometry})\;\sigma_z(x, y)\;dxdy \qquad (2.3)$$

where $\sigma_z\,(x, y)$ is the uncracked stress at the crack area locus A in the x-y plane.

$\overline{K}$ has been shown in (3) to have two equivalent definitions or interpretations. These two interpretations of $\overline{K}$ are shown in Fig. 3 for the semi-circular surface crack and in Fig. 4 for the quarter-elliptical corner crack. First $\overline{K}$ is the rms integrated average of K(s) (the specific value of K along the crack front at point (s)) over the new surface area ΔA created by selected virtual displacement* Δa of the

*Details of the prescribed crack front virtual displacement can be found in (3) and (4). It suffices to say here that more than one virtual displacement (or degree of freedom (DOF)) can be considered (as in Fig. 4) so that several growth directions and crack dimensions and associated $\overline{K}$'s can be considered simultaneously. Multiple $\overline{K}$'s decrease the error associated with averaging K(s) and allow the analyst to consider successfully such three-dimensional complications as non-self similar subcritical crack growth (refer also to (11-13). However, this paper considers the one DOF, single $\overline{K}$ $\overline{K}$ problem such as defined in Fig. 3.

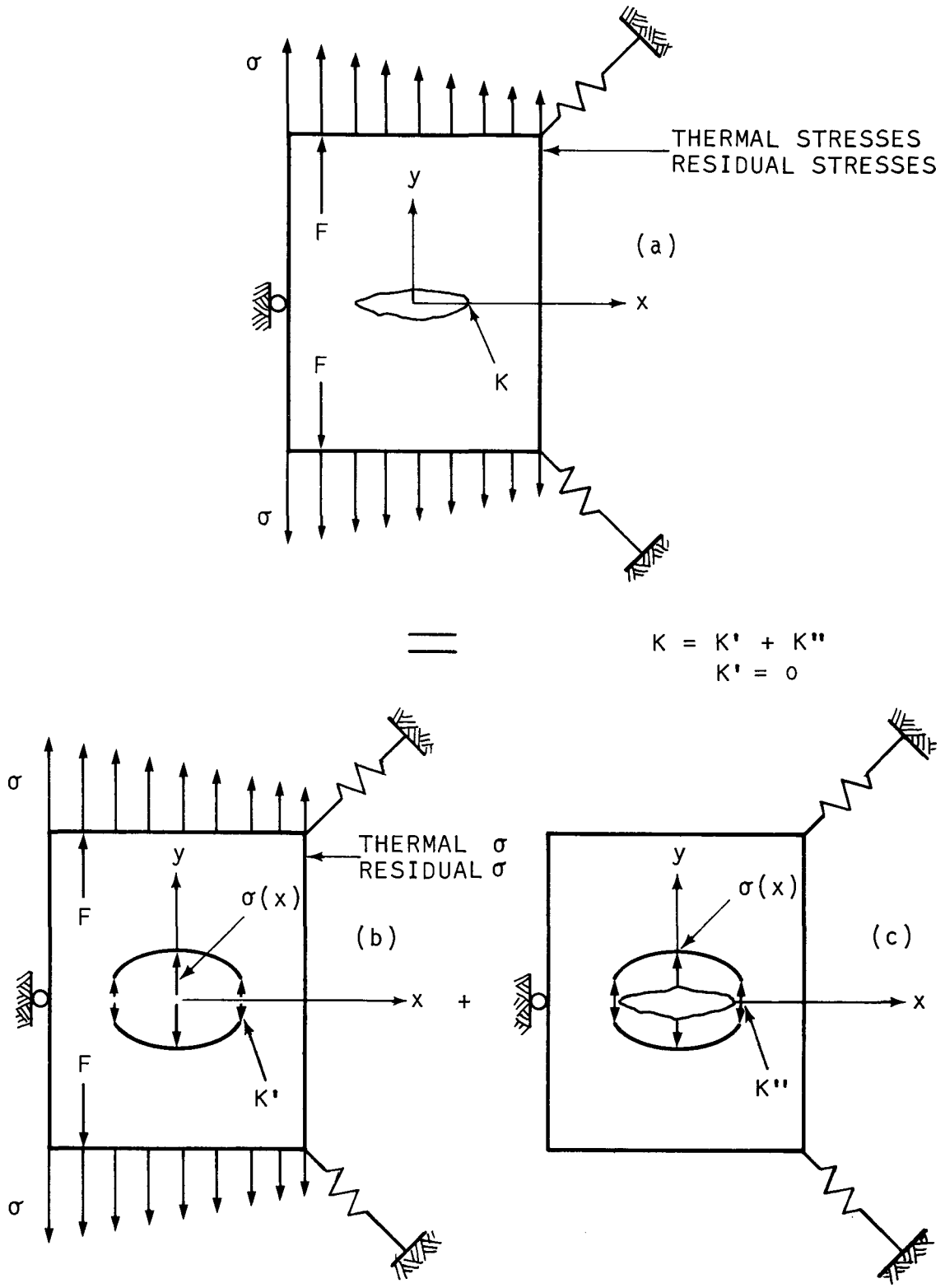

Fig. 1 - The Reduction of a Problem, (a) Into Two Simpler Problems, (b) and (c), for Computations of Stress Intensity Factor, Illustrated for a Center-Cracked Plate.

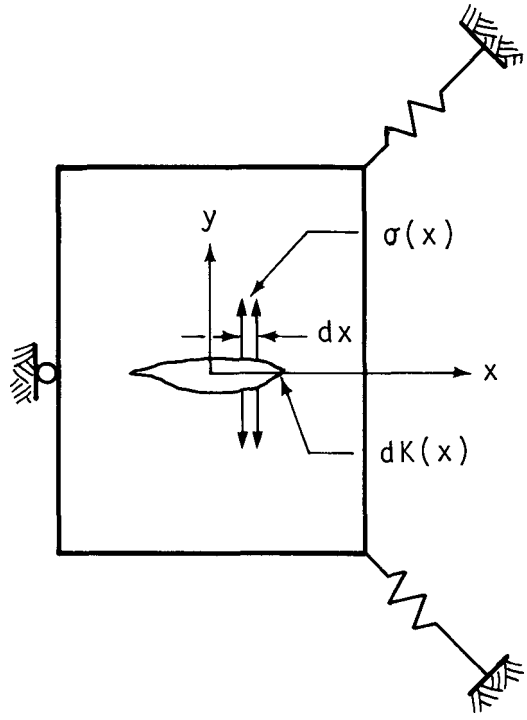

$$dK(x) = h\ (x,\ \text{GEOMETRY},\ \text{CONSTRAINTS})\ \ \sigma(x)\,dx$$

Fig. 2 - Influence Function Expression for the Stress Intensity Factor dK(x) Due to a Differential Load $\sigma(x)dx$ Applied at Crack Face Position x. Summation of dK(x) Values Over the Entire Crack Face is Used to Calculate K'' In Fig. 1c and Ultimately, the Desired Stress Intensity Factor K for the Original Structural Problem.

crack front. Second, $\overline{K}$ is also defined in the form of the strain energy release rate as

$$\overline{K}^2 = GH. \tag{2.4}$$

where,

$$H = E/(1-\nu^2) \quad \text{(plane strain case)}$$

$$E = \text{modulus of elasticity}$$

$$\nu = \text{Poisson's ratio,}$$

and, $G = \frac{\partial U}{\partial A}$ is the change in strain energy of the structure for an incremental change in crack surface area.

The key to the usage of Eq. (2.3) and, of course, to the IF method itself is the determination of h for specific cracked geometries. It is seen that h is independent of the loading and depends only on the crack face position, displacement constraints, and structural geometry. Thus, once the influence function h has been obtained for a given crack configuration, the stress intensity factor for any uncracked stress distribution may be obtained rapidly from Eq. (2.3). References (3, 4, 13) develop and apply methods to solve for h and present several three-dimensional solutions. The remainder of this section discusses the solutions (including one new result) used in the present study.

2.2 Numerical Solution of Influence Functions for the One-DOF Semi-Circular Surface Crack in a Half Space

2.2.1 Numerically-Determined Influence Functions

Reference (4) gives a detailed description of the numerical stress analysis procedures to calculate influence functions for three-dimensional

Definitions of $\overline{K}$:

1) $\overline{K}$ is the rms K value in the area $\Delta A = \pi a \Delta a$ opened by Δa. That is

$$\overline{K}^2 = \frac{1}{\Delta A} \iint_{\Delta A} K^2 (s)\, dA$$

2) $\overline{K}$ is related to the strain energy ΔU released by ΔA. That is

$$\overline{K}^2 = \frac{E}{1 - \nu^2} \frac{\Delta U}{\Delta A}$$

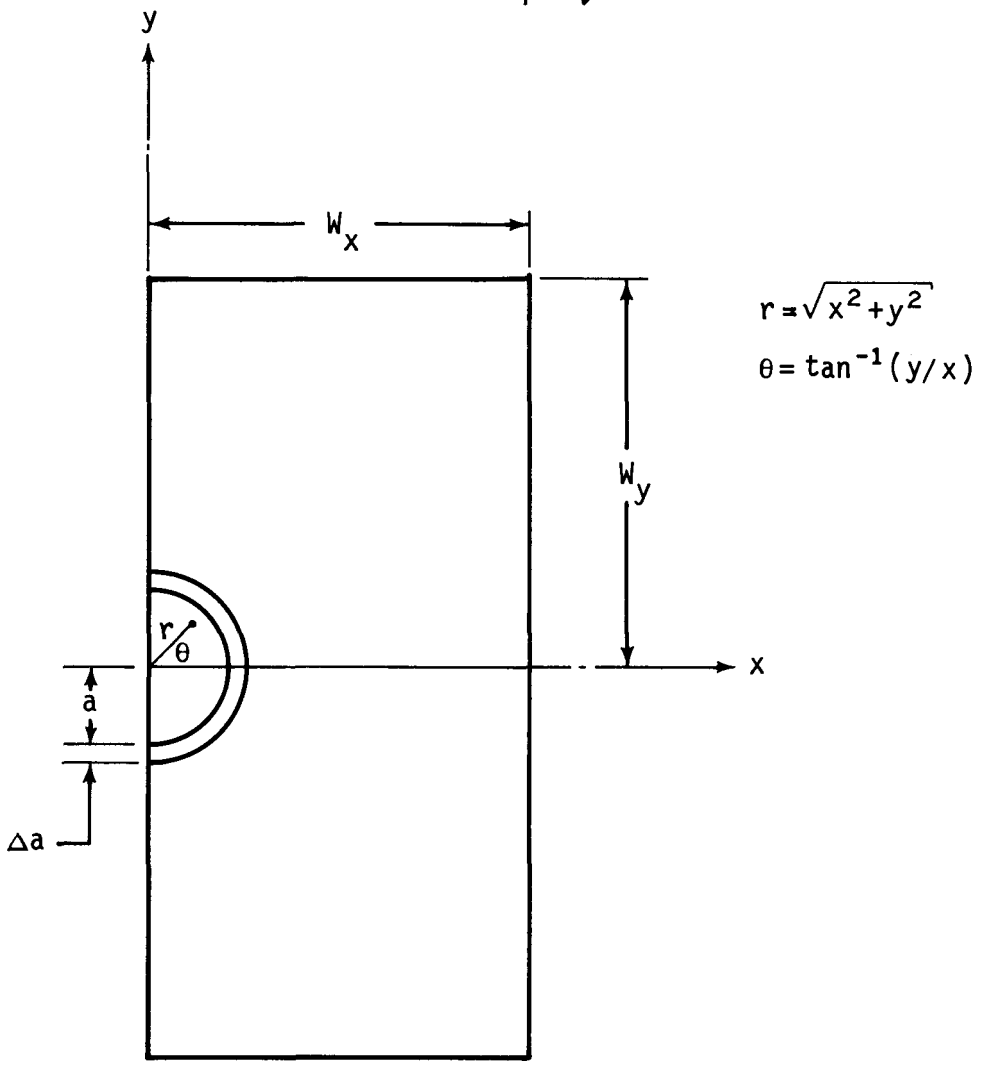

Fig. 3 - One-Degree-of-Freedom Circular Surface Crack Model Showing Two Equivalent Definitions of $\overline{K}$

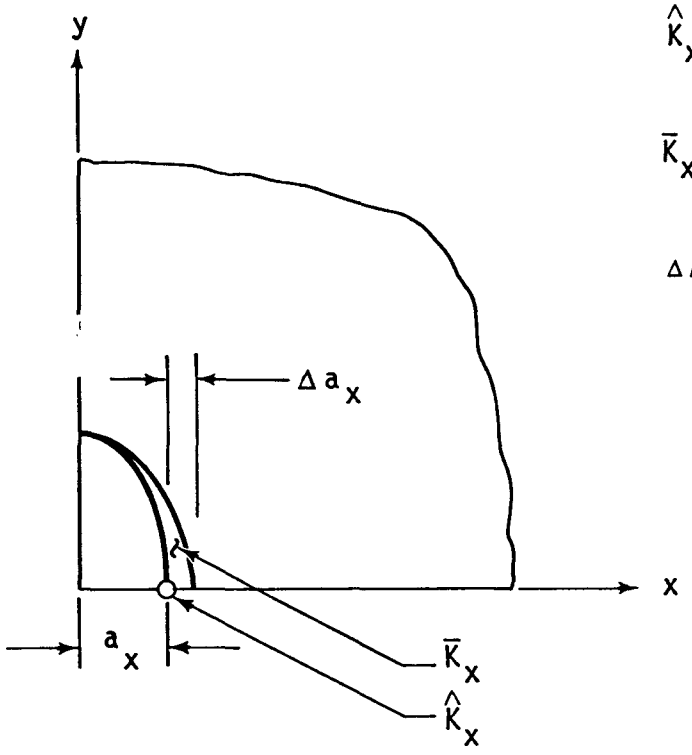

$$\hat{K}_x = K\,(a_x,\ 0)$$

$$\bar{K}_x^{\,2} = \frac{1}{\Delta A_x}\iint_{\Delta A_x} K^2(s)\,dA$$

$$\Delta A_x = \frac{\pi}{4}\, a_y\, \Delta a_x$$

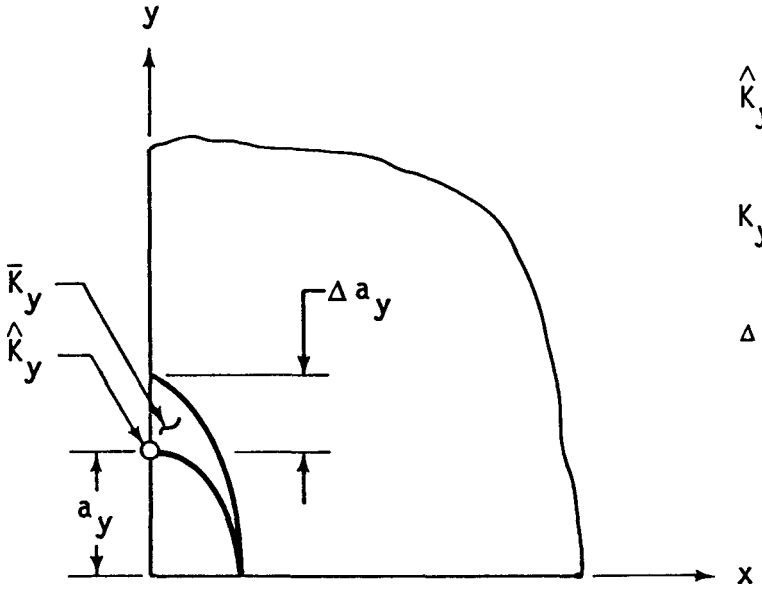

$$\hat{K}_y = K\,(0,\ a_y)$$

$$K_y^{\,2} = \frac{1}{\Delta A_y}\iint_{\Delta A_y} K^2(s)\,dA$$

$$\Delta A_y = \frac{\pi}{4}\, a_x\, \Delta a_y$$

FIG. 4 - Two-Degree-of-Freedom Elliptical Corner Crack Model.

crack problems. Essentially,h is obtained from the relationship

$$h = \left[\frac{1}{H} \quad \frac{\partial U}{\partial A} \right]^{-1/2} \quad \frac{\partial w^*}{\partial A} \tag{2.5}$$

where

$$H = \begin{cases} \dfrac{E}{1-\nu^2} & \text{for plane strain} \\ E & \text{for plane stress} \end{cases}$$

U = strain energy

w^* = crack opening displacement

A = crack area

The values of U and w* are obtained for a simple loading condition (e.g., uniform crack face pressure in this study) using the boundary integral equation (BIE) method (26). Finite element, finite difference or experimental techniques could have been used to solve the uniform pressure problem also. Reference (13) applies BIE and various numerical procedures to calculate influence functions using (2.5) for the subject problem (Fig. 3). The resulting solution is given by

$$h(a, x, y) = 2\ (\pi a)^{-3/2}\ (1-R^2)^{-1/2}\ f\ (R,\theta) \tag{2.6}$$

where

a = radius of semi-circular crack centered at the origin in the x-y plane

$$R = r/a \tag{2.7}$$

$$r = (x^2 + y^2)^{1/2}$$

$$\theta = \arctan(x/y)/(\pi/2) \tag{2.8}$$

$$f(R,\theta) = C\left\{a_0 + b_1 + b_2 - (1-R^2)\ (1.5b_1 + 2.5b_2)\right\}. \tag{2.9}$$

Furthermore,

$$b_1 = a_1 R^{1.5} \theta^{0.15} + a_2 R^{1.5} \theta^{0.30}$$
$$b_2 = a_3 R^{2.5} \theta^{0.15} + a_4 R^{2.5} \theta^{0.30} \qquad (2.10)$$

and

$$C = 0.92755 \qquad a_2 = -1.52517$$
$$a_0 = 1.30957 \qquad a_3 = 0.88531 \qquad (2.11)$$
$$a_1 = 0.75531 \qquad a_4 = 1.3767$$

As described in detail in (3), the function $f(R,\theta)$ is evaluated by multi-parameter curve fitting of crack-opening displacements calculated from two full three-dimensional analyses of a buried circular crack and of the Fig. 3 geometry, both with uniformly pressurized cracks. A boundary integral equation (BIE) method computer program (14) is used for the three-dimensional crack analysis. The BIE method for mixed boundary value problems (6, 14-17, 26) consists of a numerical solution of an integral equation relating the boundary tractions and the boundary displacements. In all but the simplest of cases the integral equation must be solved numerically for the unknown boundary data. However, only the surface of the body is discretized in order to perform the numerical integrations, thus reducing the dimensionality of the problem by one and resulting in more efficient and accurate solutions than obtainable with FE for certain crack problems. Figures 5a, 5b, 5c and 6 show the boundary discretizations and conditions used to obtain crack opening displacements for embedded, surface, and corner circular cracks under uniform crack face pressure. The actual errors in the calculated crack opening displacements

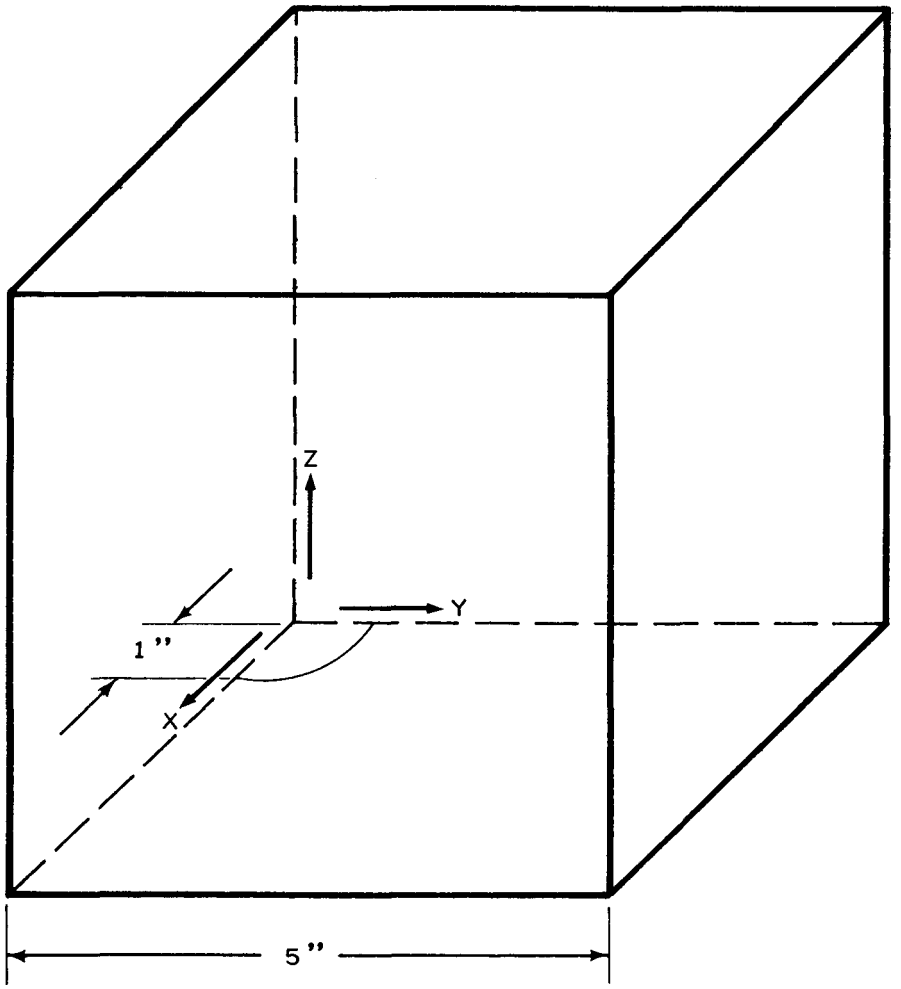

Fig. 5a - BIE Circular Crack Model (5" Cube Satisfactorily Models An Infinite Media For the 1" Radius Crack).

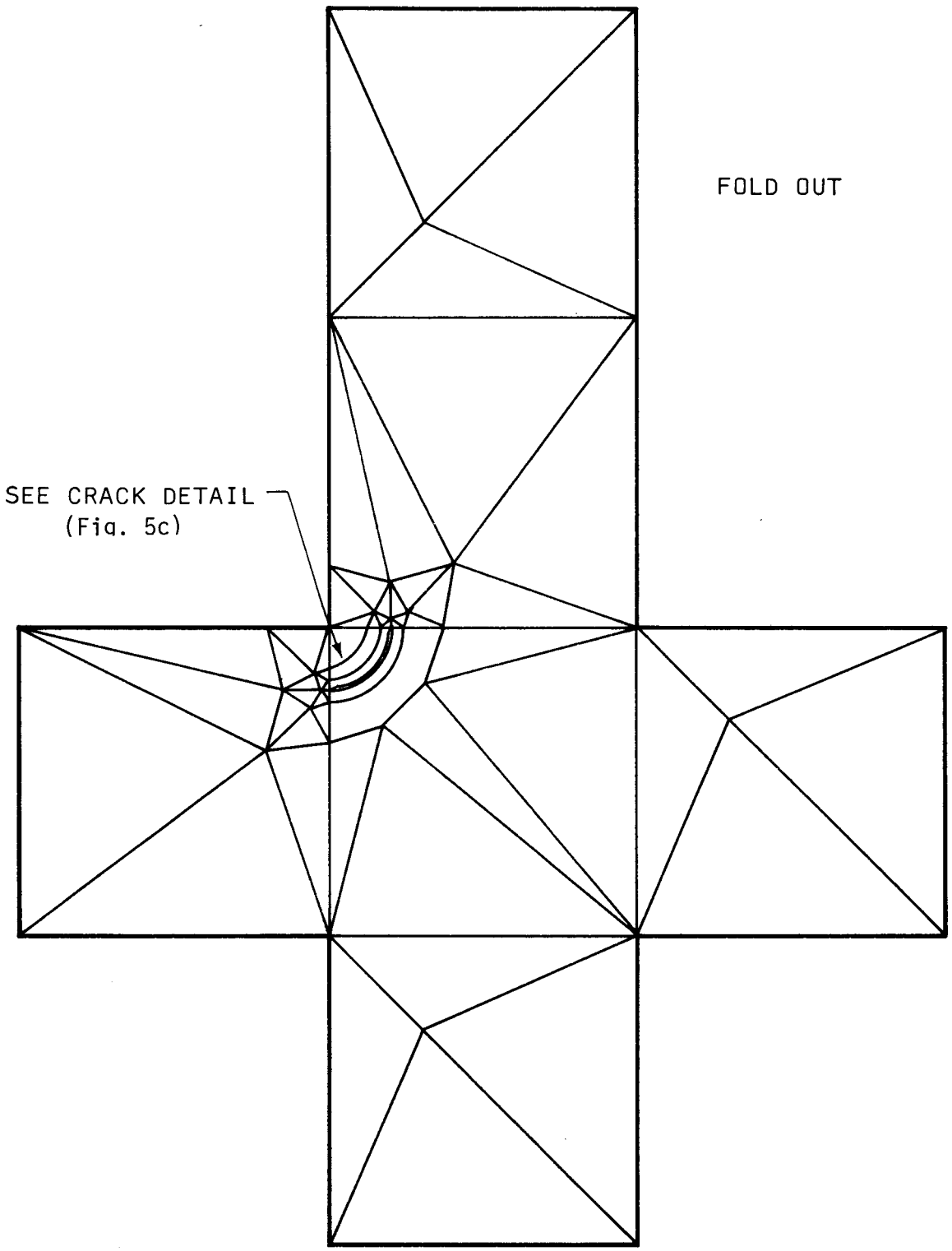

FIG. 5b - BIE Boundary Segment Model for Circular Crack Programs

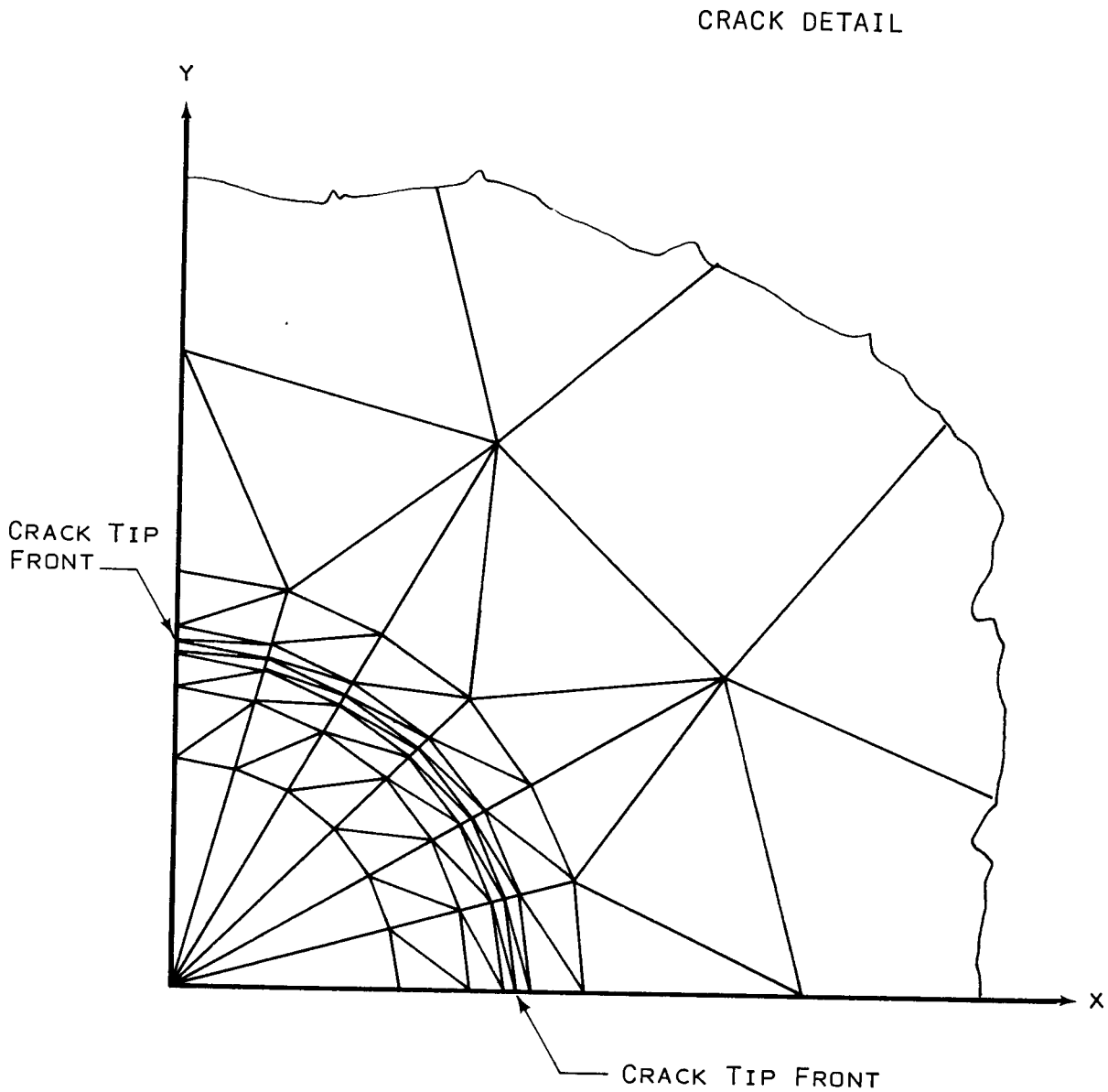

FIG. 5c - Details of BIE Boundary Segment Model in the Plane Vicinity of the Circular Crack.

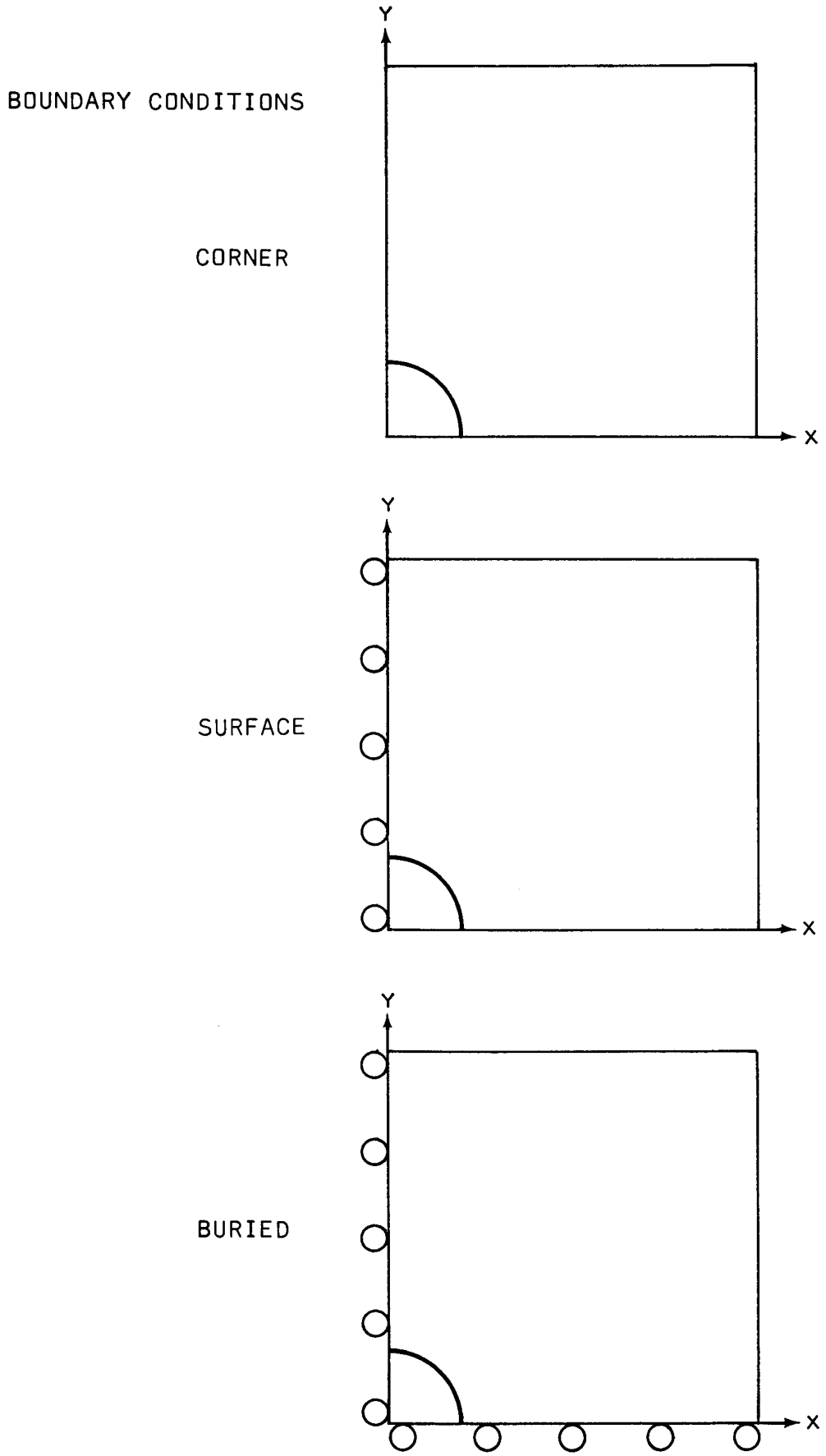

FIG. 6 - BIE Boundary Conditions for Circular Crack Problems

range between -1% and -7% and have been shown (26) by repeated numerical experiment and comparison with more accurate solutions to be systematic functions of crack face position. It is speculated that embedded and surface crack displacements have similar errors because the error is more a function of boundary descretization than boundary conditions. Thus, these known error trends can be accounted for by normalizing with respect to the published exact embedded crack solutions (3, 6, 26), and the effective error range of the resulting normalized displacements has been reduced to approximately $\pm$ 1.5% (26). The normalization is performed by computing the crack opening displacements $u_z(x,y)$ with the BIE method for both the embedded crack problem and the surface crack problem. The numerical surface crack displacements are then "improved" by utilizing the formula

$$(u_{z\text{-surface}})_{\text{improved}} = \frac{(u_{z\text{-embedded}})_{\text{exact}}}{(u_{z\text{-embedded}})_{\text{BIE}}} (u_{z\text{-surface}})_{\text{BIE}} \quad (2.12)$$

The details, accuracy, cost, and convenience advantages of the BIE method are well documented in (14-17). Each of the two solutions (surface and embedded cracks) required 12 minutes of CPU time, costing about $54 on an IBM 360/67 computer.

The stress intensity factors for the surface crack are computed by substitution of h into

$$\overline{K} = \iint h(a, x, y)\sigma_z(x, y)\, dxdy. \quad (2.13)$$

2.2.2 Accuracy and Finite Width Limitations

The half-space, infinite body stress intensity factor solution presented above is accurate (18-21) to within 3% for the finite body

problems in Fig. 3 for the cases:

$$1)\ a/W_x < 0.6 \qquad (2.14)$$

$$W_z \to \infty$$

$$2)\ a/W_y < 0.6 \qquad (2.15)$$

$$W_x \to \infty$$

$$3)\ a/W_x < 0.5 \qquad (2.16)$$

$$a/W_y < 0.5$$

where W_x, W_y are width dimensions defined in Fig. 3.

Eqn. (2.13) is evaluated numerically using a rectangular partitioning scheme with a refined grid near the crack front ($R \to 1$), to account for the $(1-R^2)^{-1/2}$ singularity of h.

2.3 Other Influence Functions Used in This Study

Influence functions for two additional one-DOF geometries have been utilized in this study. The geometries are a circular buried crack in an infinite space (Fig. 7) and a quarter-circle corner crack in a quarter-space (Fig. 8).

2.3.1 Buried Circular Crack

The exact circular crack influence functions to compute $\bar{K}$ are derived in (13) as

$$h(a, x, y) = (\pi a)^{-3/2} (1-R^2)^{-1/2} \qquad (2.17)$$

and the stress intensity factor is

$$\bar{K} = \iint h(a, x, y)\, \sigma_z(x,y)\, dxdy \qquad (2.18)$$

Eqn. (2.18) is evaluated numerically with the same analysis techniques as used for Eqn. (2.13).

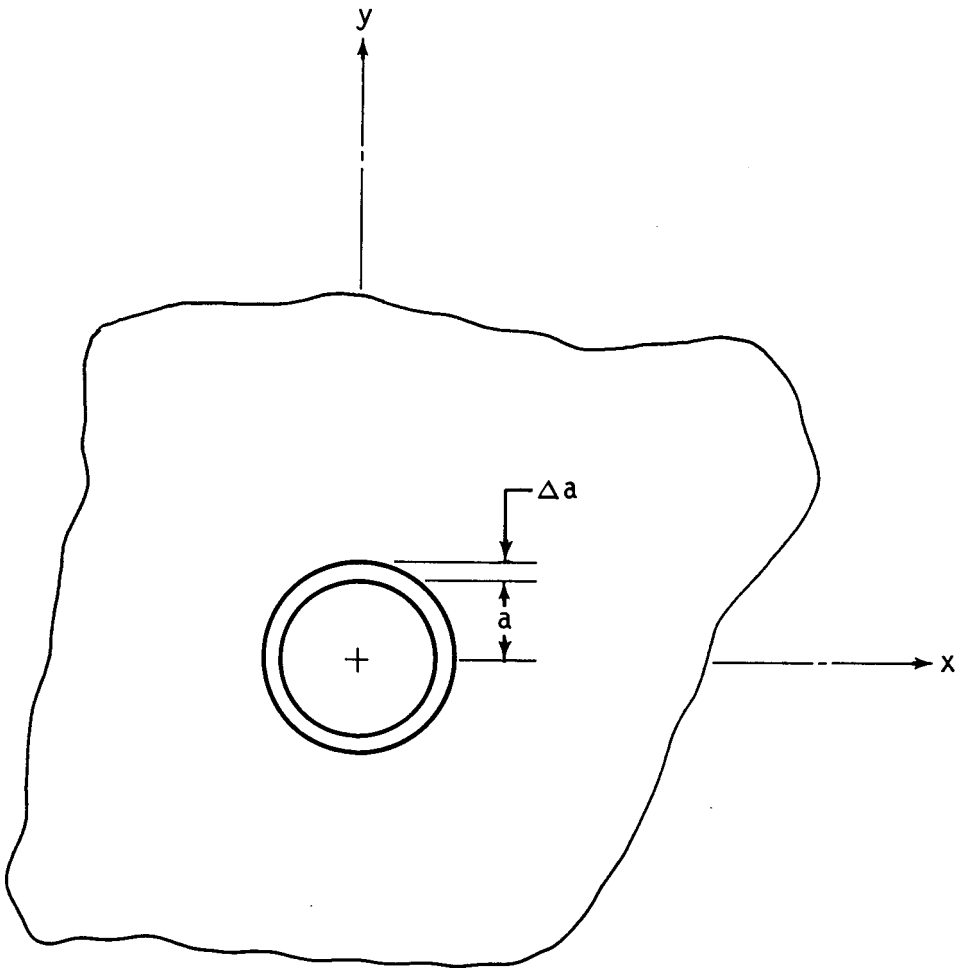

$$\overline{K}^2 = \frac{1}{\Delta A}\iint_{\Delta A} K^2\,(s)\,dA = \frac{E}{1-\nu^2}\,\frac{\Delta U}{\Delta A}$$

$$\Delta A = 2\,\pi a\,\Delta a$$

Fig. 7 One-Degree-of-Freedom Circular Crack in an Infinite Solid

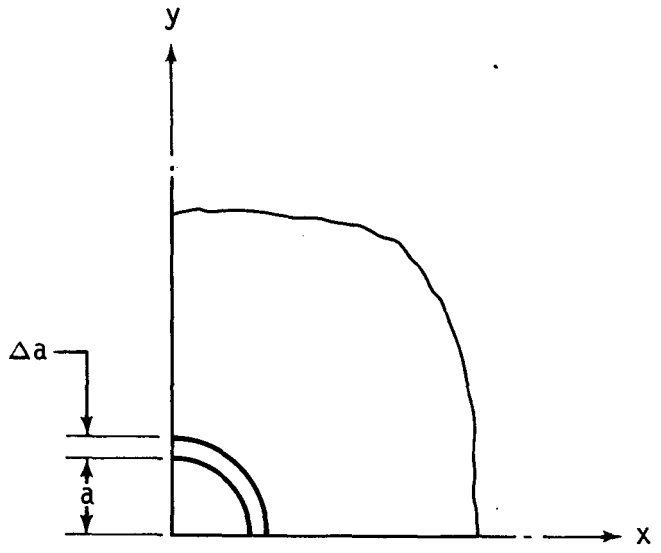

$$\overline{K}^2 = \frac{1}{\Delta A}\iint_{\Delta A} K^2\,(s)\,dA = \frac{E}{1-\nu^2}\,\frac{\Delta U}{\Delta A}$$

$$\Delta A = \frac{\pi}{2}\,a\,\Delta a$$

Fig. 8 One-Degree-of-Freedom Quarter-Circular Corner Crack in a Quarter-Space

2.3.2 One-DOF Quarter-Circular Crack in a Quarter Space

References (6, 13) obtain numerical solutions for two stress intensity factors $\bar{K}_x$ and $\bar{K}_y$ for a two-DOF quarter-ellipse corner crack problem in Fig. 4. This solution is easily degenerated to the desired solution of the subject problem by first computing $\bar{K}_x$ and $\bar{K}_y$ for the two-DOF quarter-circle crack and then obtaining the one-DOF solution $\bar{K}$ from

$$\bar{K} = (\bar{K}_x^2 + \bar{K}_y^2)^{1/2} \tag{2.19}$$

The elliptical crack solution in (13) required eight full three-dimensional BIE crack analyses to account for various aspect ratios of the minor and major elliptical axes. The boundary discretization and boundary conditions used were identical to those shown in Figs. 5a, 5b, 5c and 6 except that the circular crack was mapped into elliptical shapes (13). Again, each of the eight analyses required 12 minutes of CPU time on an IBM 360/67 computer, at a cost of $54.

3.0 FINITE ELEMENT STRESS INTENSITY FACTOR COMPUTATIONS

This section summarizes the methods given for direct finite element (FE) analysis of three-dimensional crack problems. The strain energy release rate method is used to compute the stress intensity factor K from the results of finite element analyses of the crack geometry under the actual or simulated thermo-mechanical loading. Strain energy, U, is calculated for a set of discrete circle sizes, a_i; then standard central and backward difference expressions are applied to estimate $\partial U/\partial a$ from the set $U(a_i)$. K is calculated from Eqn. (2.4) which is repeated below for convenience.

$$K^2 = \bar{K}^2 = GH = \frac{\partial U}{\partial a}\frac{\partial a}{\partial A} H \qquad (3.1)$$

According to (2), if special crack tip elements are not used, this is the most economical of the various finite element methods for fracture mechanics analysis and is required by the large number of elements needed to model the nozzle. It is also the most feasible method when a number of different crack sizes are to be investigated. The main drawbacks result from the fact that only an average value of K can be obtained* and, of course, from the expense inherent in any full three-dimensional finite element analysis.

3.1 Finite Element Computer Program Selection and Modifications

The ANSYS computer program (22) was selected for three-dimensional thermo-mechanical stress analysis, with and without the crack. Three-dimensional, elastic, octahedral isoparametric and triangular constant strain elements were used in all cases. Preliminary uncracked stress analyses were used to

*As with the IF method, several $\bar{K}$'s can be computed with FE, each corresponding to a local average of K(s) at some crack front position. References (3,4) provide additional details.

verify the ability of the program to calculate strain energy for thermal problems and the uncracked thermal stress distribution required for application of the IF method.

3.2 Crack Problem Modeling, Discretization and Solution Procedure

Figures 9, 10a, 10b and 10c illustrate as an example the crack model of one of the test cases to be discussed in Section 4, a semi-circular surface crack in semi-infinite (i.e., large rectangular) solid. Symmetry considerations are used where applicable to reduce the size of all models so that only 1/4 of the structure in Fig. 9 need be modeled. Figures 10a-10c illustrate the relatively coarse discretization used to reduce further the problem size.

The method used for determining stress intensity factors is outlined as follows:

1. Construct a finite element model of the structure using a mesh which will provide for a series of uniform increments of crack enlargement.

2. Apply correct loading and boundary conditions and run uncracked case.

3. Compute (or read) total strain energy.

4. Release first set of nodes (resulting in first crack size as given by radius a) and run,

5. Compute (or read) total strain energy.

6. Repeat 4 and 5 for successive increasing crack sizes.

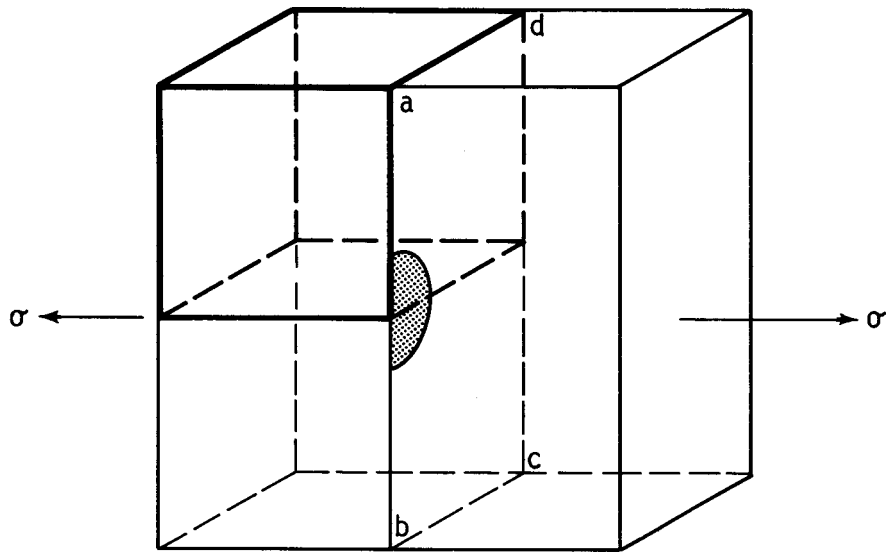

PLANE (a b c d) CONTAINS CRACK.

Fig. 9 Semicircular Surface Crack; Semi-infinite Solid; Uniform Tension

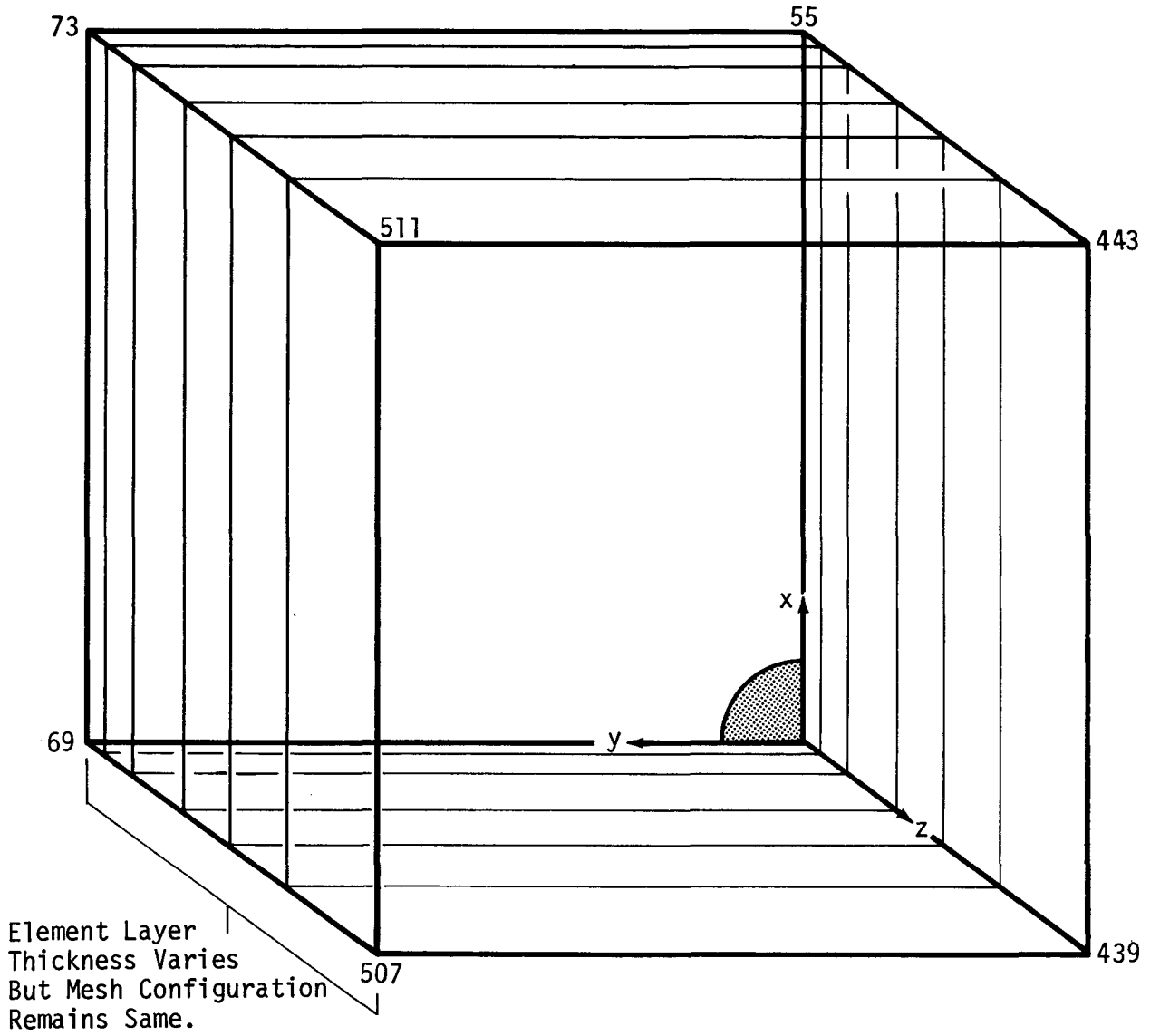

Fig. 10a Finite Element Computer Model - Basic Configuration
Showing Element & Nodal Layers

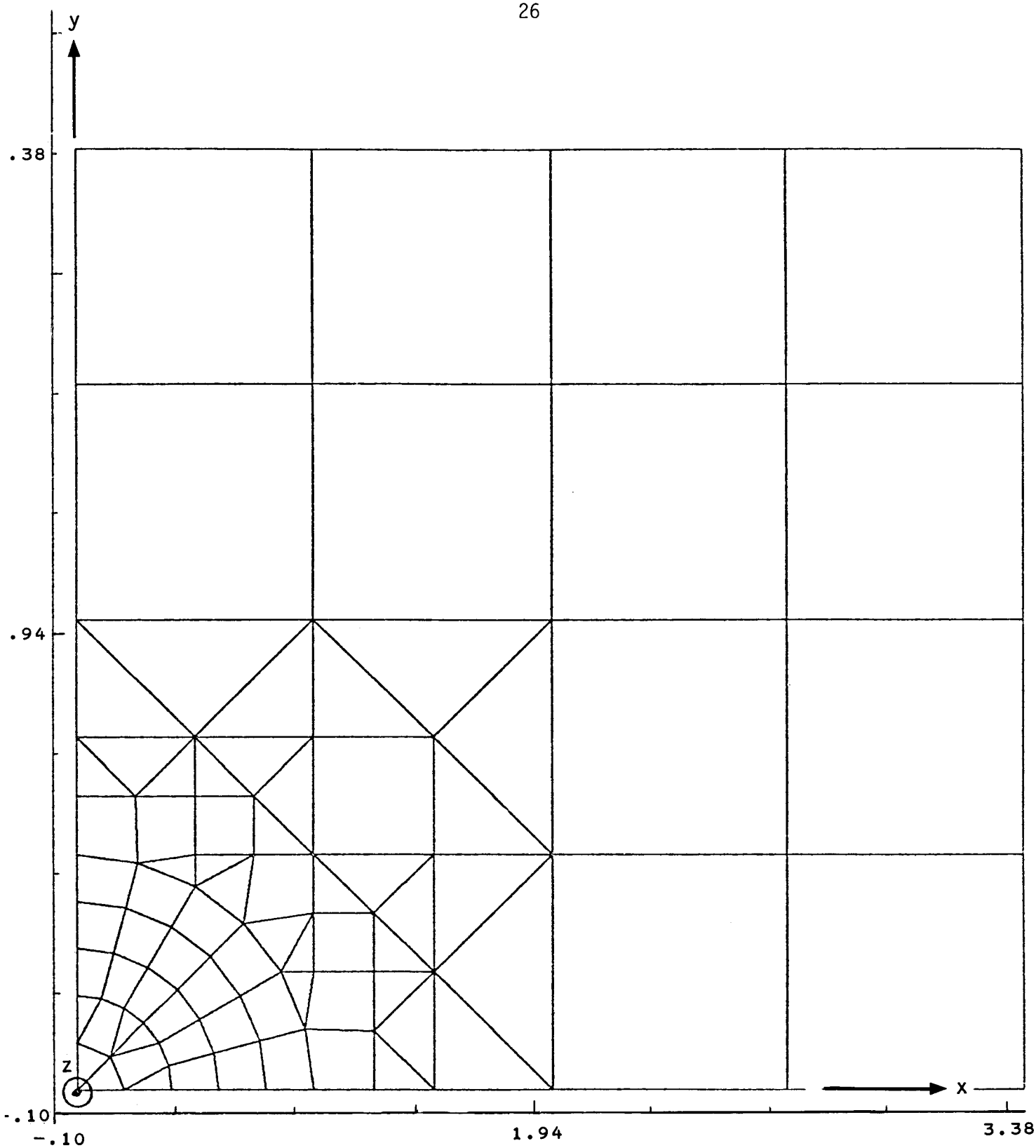

Fig. 10b Finite Element Model Used for Semicircular Crack Cases;
View Along Z-Axis, Typical Element Layer (Same Mesh Size Used for All Layers)

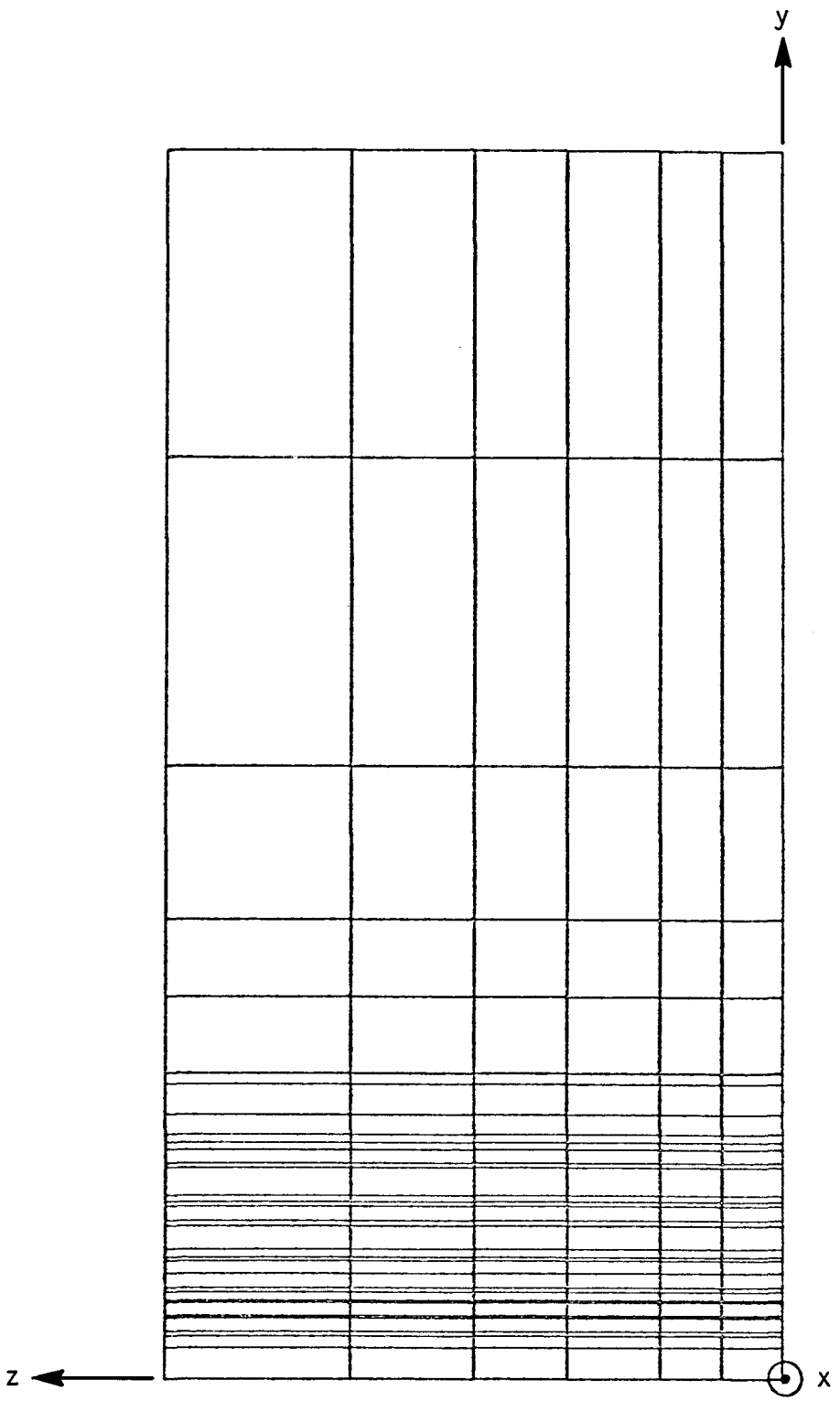

Fig. 10c Discretization of Side of Model Showing Layered Structure (Vertical Lines Only).

(View Along y-axis is Similar to View Along x-axis Shown Above.)

7. Obtain curve or table of strain energy vs. crack radius a. It has been noted in a previous similar study(10)that the strain energy release rate method gives best results when the crack tip is assumed to be located at the centroid of the element adjacent to the model crack tip. The finite element results herein are also based on this procedure.

8. Determine $\partial U/\partial a$ using finite difference or curve fit technique.

9. Compute stress intensity factor: $\bar{K}^2 = \left(\frac{E}{1-\nu^2}\right)\left(\frac{\partial U}{\partial a}\right)\left(\frac{2}{\pi a}\right)$ where $dA = (\pi a/2)\, da$ is the increment of crack area for a quarter-circular crack.

4.0 RESULTS OF STRESS INTENSITY FACTOR TEST CASE SOLUTIONS

4.1 Selected Test Cases

Eight test cases and models were chosen on the basis of there being an accurate published solution available using some third method of solution, and also to reflect, as nearly as possible, the crack geometries and mesh size to be used in the nozzle model. The eight selected test cases are listed in Table I along with reference numbers of published K solutions, error estimates of published solutions, and numbers of the figures that illustrate the test cases and present stress intensity factor results. The first five test cases were used in the comparative study of the IF and FE methods while the last three cases are chosen to provide additional verification of the IF method. Table II and Figs. 11-18 present detailed calculation results for the individual test cases. Table III summarizes cost and accuracy data for all selected test cases.

4.2 Results of Three Test Cases for Circular-Shaped Cracks Under Uniform Stress

Figure 11 illustrates the stress intensity factor results obtained from three solutions of the problem of a circular crack embedded in a comparatively large solid under remote uniform tensile stress. Similarly, Figs. 12 and 13 illustrate the solutions obtained for a semi-circular surface crack and quarter-circular corner crack in large bodies under remote normal uniform tension. As shown, the finite element method tended to give stress intensity factor results that were too large in the range of crack size radius "a" of 0 to .6 inches. For a larger than .6 inches using the discretization of Fig. 10, the finite element results tended to cross the curve for the accurate published solutions. In general, as shown in

TABLE I

SELECTED TEST CASES FOR ACCURACY AND COST EVALUATION
OF THE IF AND FE METHODS OF THREE-DIMENSIONAL ELASTIC STRESS ANALYSES OF CRACKS

NUMBER	TEST CASE DESCRIPTION	MODEL SKETCH	FIG. OR TABLE NUMBERS FOR: RESULTS OF TEST CASE	REF. NUMBER OF BEST AVAIL. PUB. SOLUTION	EST. ERROR OF PUB.SOLUTION
1.	Circular embedded crack in an infinite solid; a uniform tensile stress field in the body, normal to the crack faces	6,7	11	20	0
2.	Semi-circular surface crack in a semi-infinite solid; uniform tensile stress field.	3,6b,9,10	12	6,25	±2%
3.	Quarter-circular corner crack in a quarter-infinite solid; uniform tensile stress field.	6a, 8	13	6,25	±2%
4.	Semi-circular surface crack in a semi-infinite solid; complex thermal loading.	3,14	15,17	N/A	N/A
5.	Additional thermal loading case.	3,14	16,18	N/A	N/A
6.	Circular embedded crack in an infinite solid; a radially decreasing tensile stress distribution normal to the crack plane.	Table II	Table II	20	0
7.	Circular embedded crack in an infinite solid; a radially increasing tensile stress distribution normal to the crack plane.	Table II	Table II	20	0
8.	Quarter-circular corner crack; parabolic tensile stress normal to the crack plane.	3	19	19	±5%

*Published solutions are authoritative, but do not necessarily contain the original published solution.
N/A - Not applicable since no published solution is available for specific thermal loading.

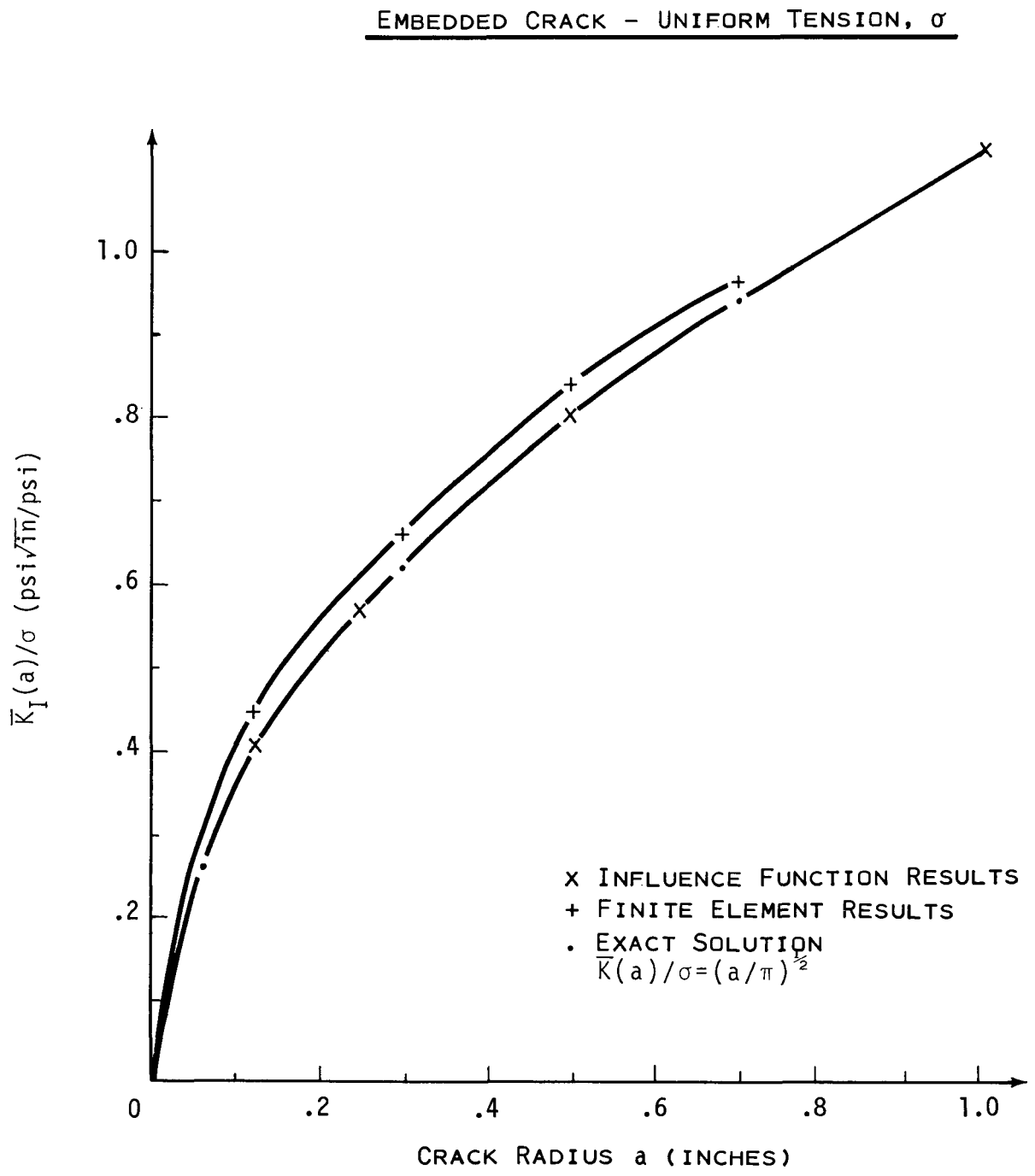

Fig. 11 Comparison of Stress Intensity Factors Calculated With Influence Functions, Finite Elements, and the Exact Solution $\bar{K}_I(a) = 2\sigma(a/\pi)^{1/2}$ For Embedded Circular Crack Under Uniform Tension, σ.

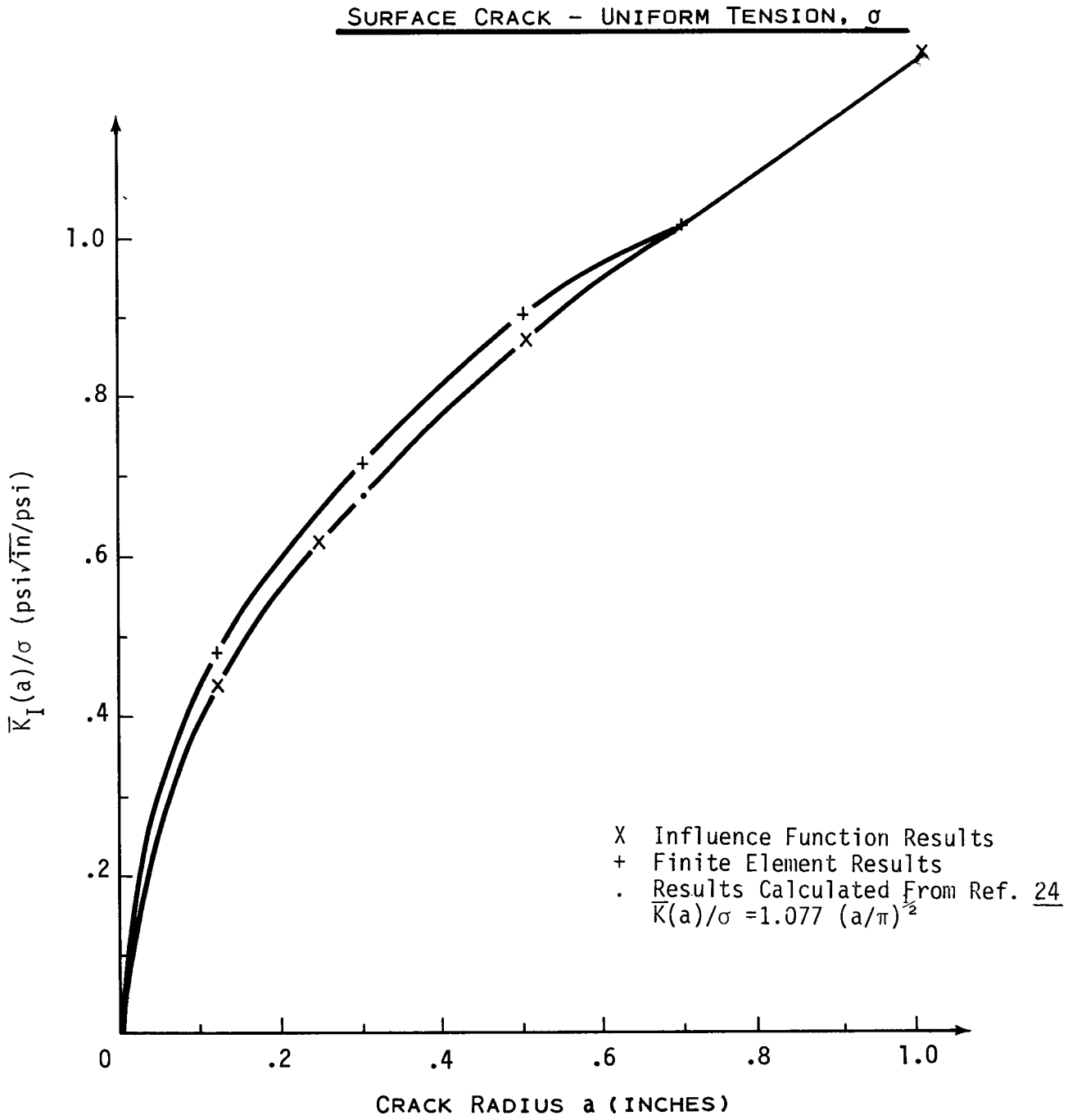

Fig. 12 Comparison of IF, FE, and Published Results For Semicircular Surface Crack Under Uniform Tension

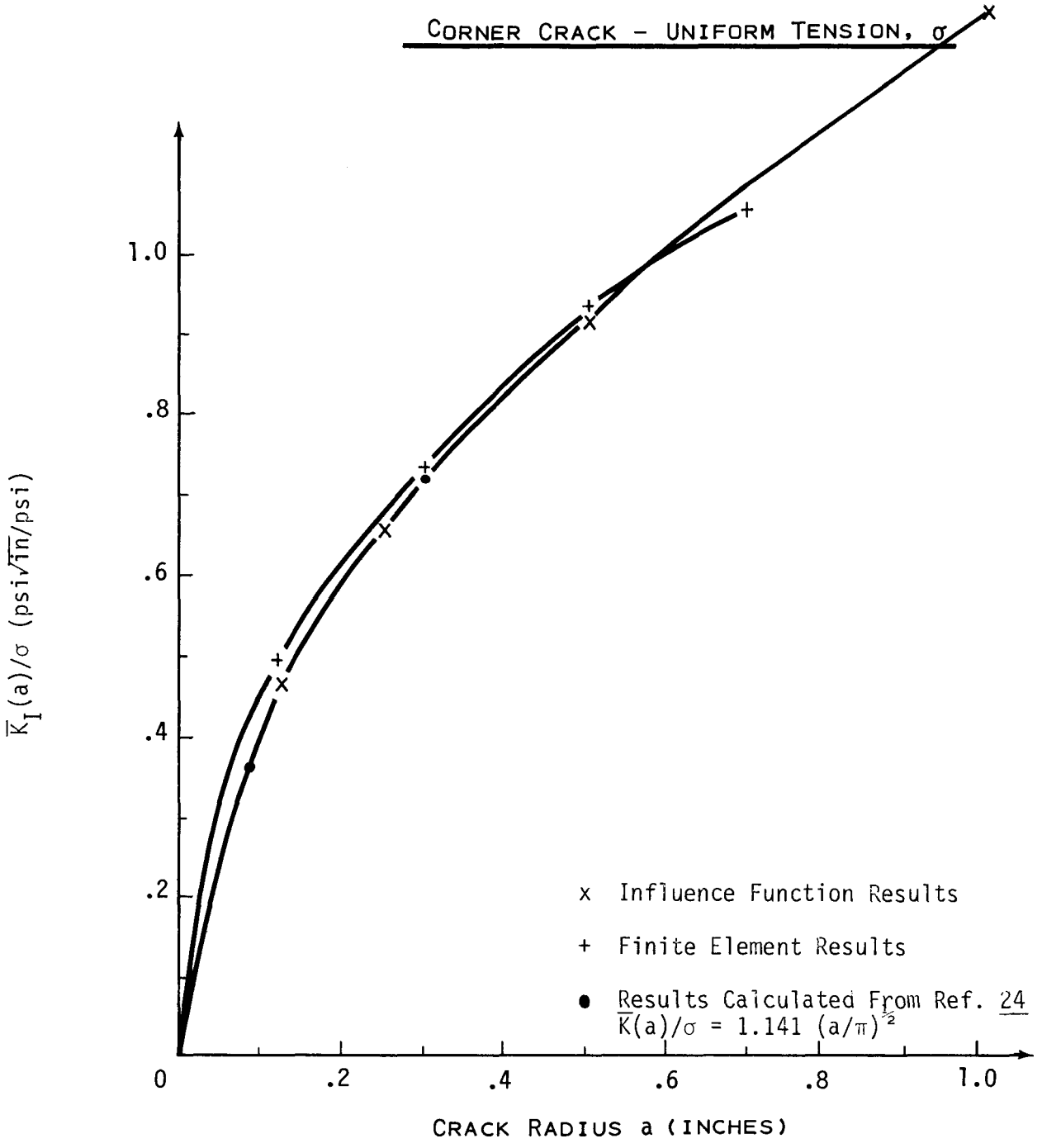

Fig. 13 Comparison of IF, FE, and Published Results For Quarter-Circular Corner Crack Under Uniform Tension

Figs. 11-13, the IF results were nearly identical to the accurate published results with the largest errors equal to +0.7%, the value observed for the embedded circular crack test case.

4.3 Results of Semi-Circular Surface Crack Test Cases For Two Complex Thermal Loadings

Figure 14 is a schematic representation of a complicated thermal stress field being applied to a large solid with a semi-circular surface crack. Figures 15 and 16 show the two normalized design-based BWR nozzle thermal loadings used for the two thermal test cases. These figures demonstrate that the finite element analysis accurately calculates distribution of thermal stresses in the uncracked solid. Figures 17 and 18 show the stress intensity factor results obtained for the thermal loading problems using three methods: the FE method, the IF method, and an approximate technique discussed earlier in the introduction, given in the ASME Boiler and Pressure Vessel Code, Section XI (1). As seen from Figs. 17 and 18, the IF and FE results are in reasonable agreement. The Code results have significant errors (differences) when compared to the more accurate techniques recommended by the present authors. Although no accurate stress intensity factor solution was available using some acceptable third method of solution, we infer from the agreement between the IF and FE methods in Test Cases 4 and 5 (and from the success of both methods in Test Cases 1-3) that both techniques are capable of obtaining reasonably accurate solutions to these complex thermal stress crack problems.

4.4 Discussion of Finite Element Results for the First Five Test Cases

It has been demonstrated in five test cases that reasonably accurate stress intensity factors may be computed from a coarse mesh finite element

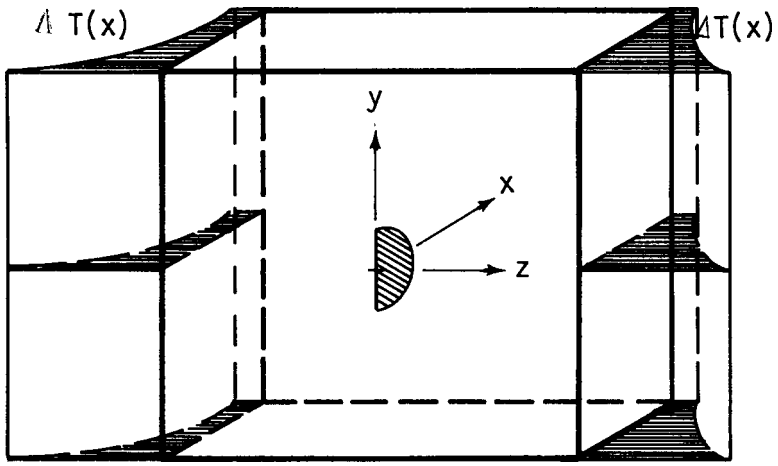

Fig. 14 - Surface Crack Under High-Gradient Thermal Loading

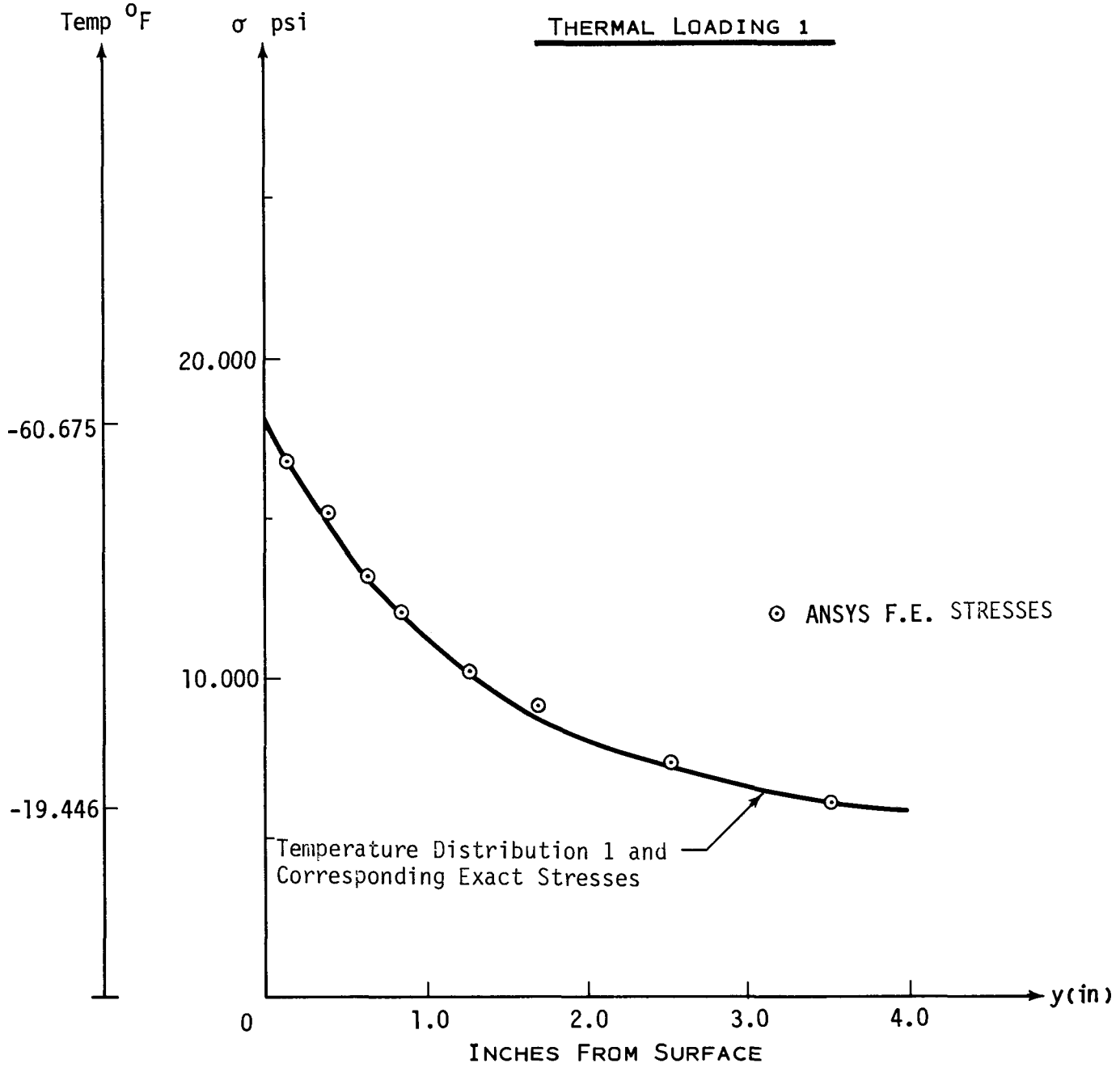

Fig. 15 - Uncracked Thermal Stress Due to Temperature Distribution 1

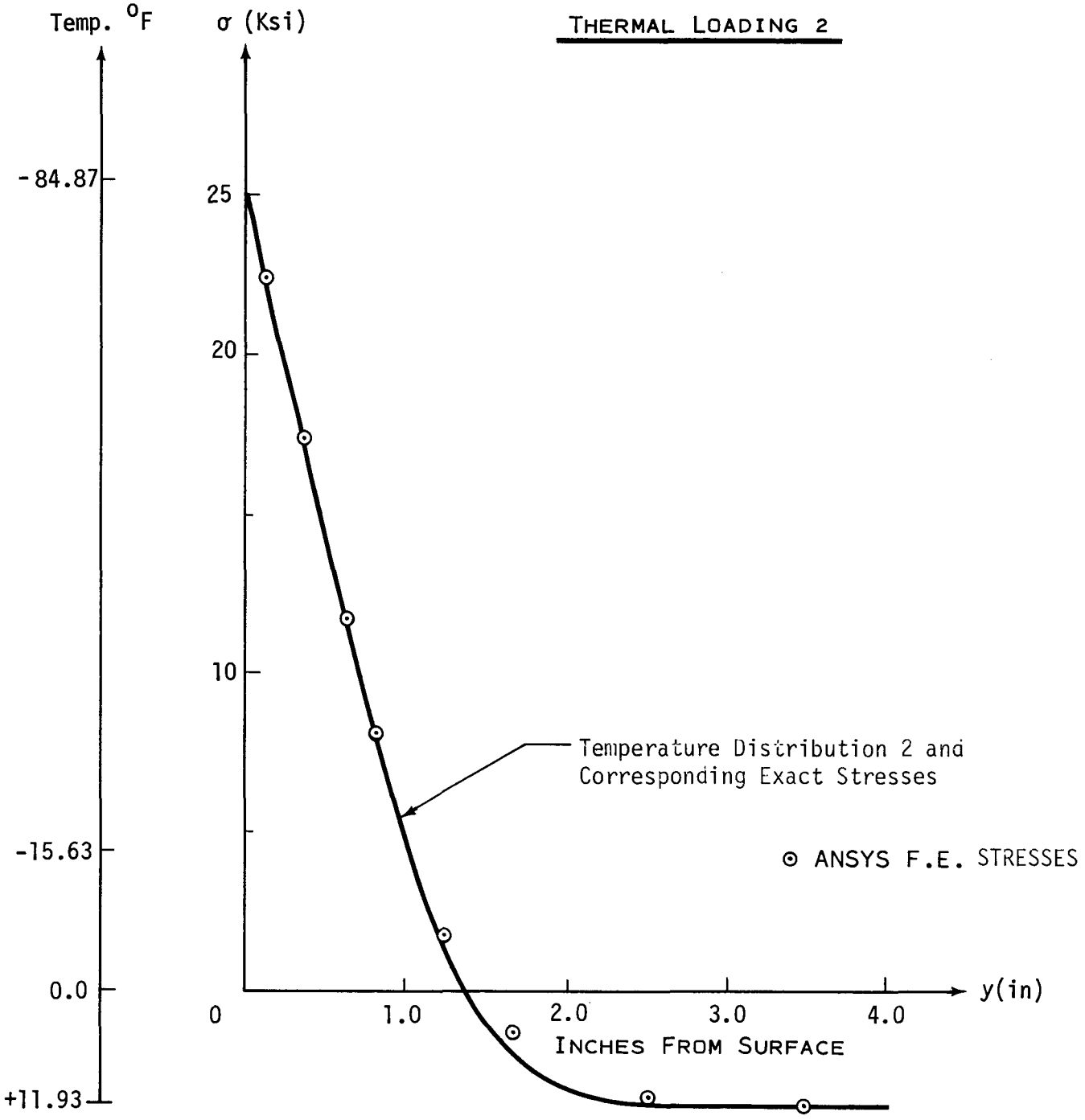

Fig. 16 - Uncracked Thermal Stress Due to Temperature Distribution 2

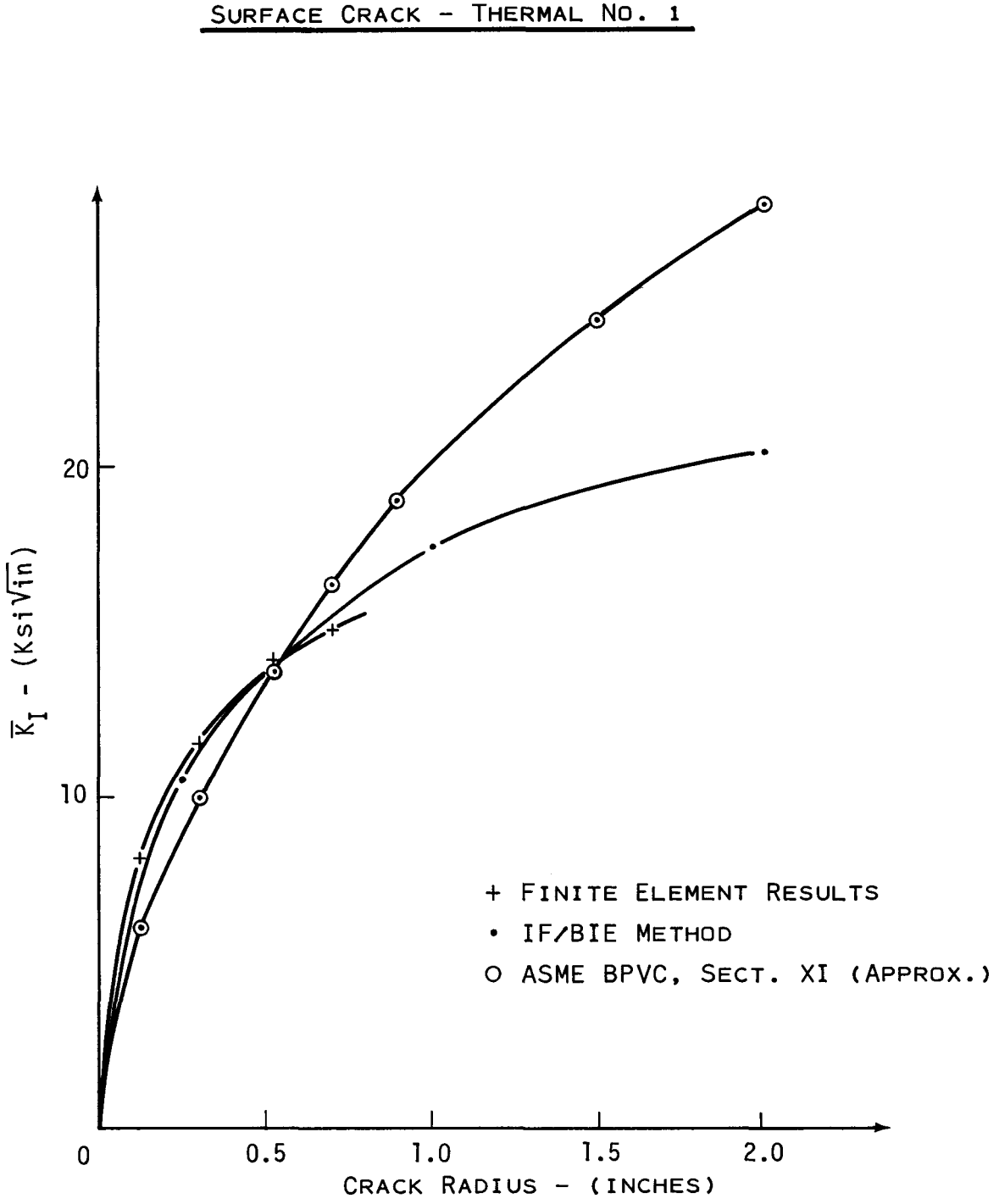

Fig. 17 - Comparison of FE, IF, and ASME Code Section XI Methods to Compute $\bar{K}(a)$ for a Surface Crack Under Thermal Loading 1.

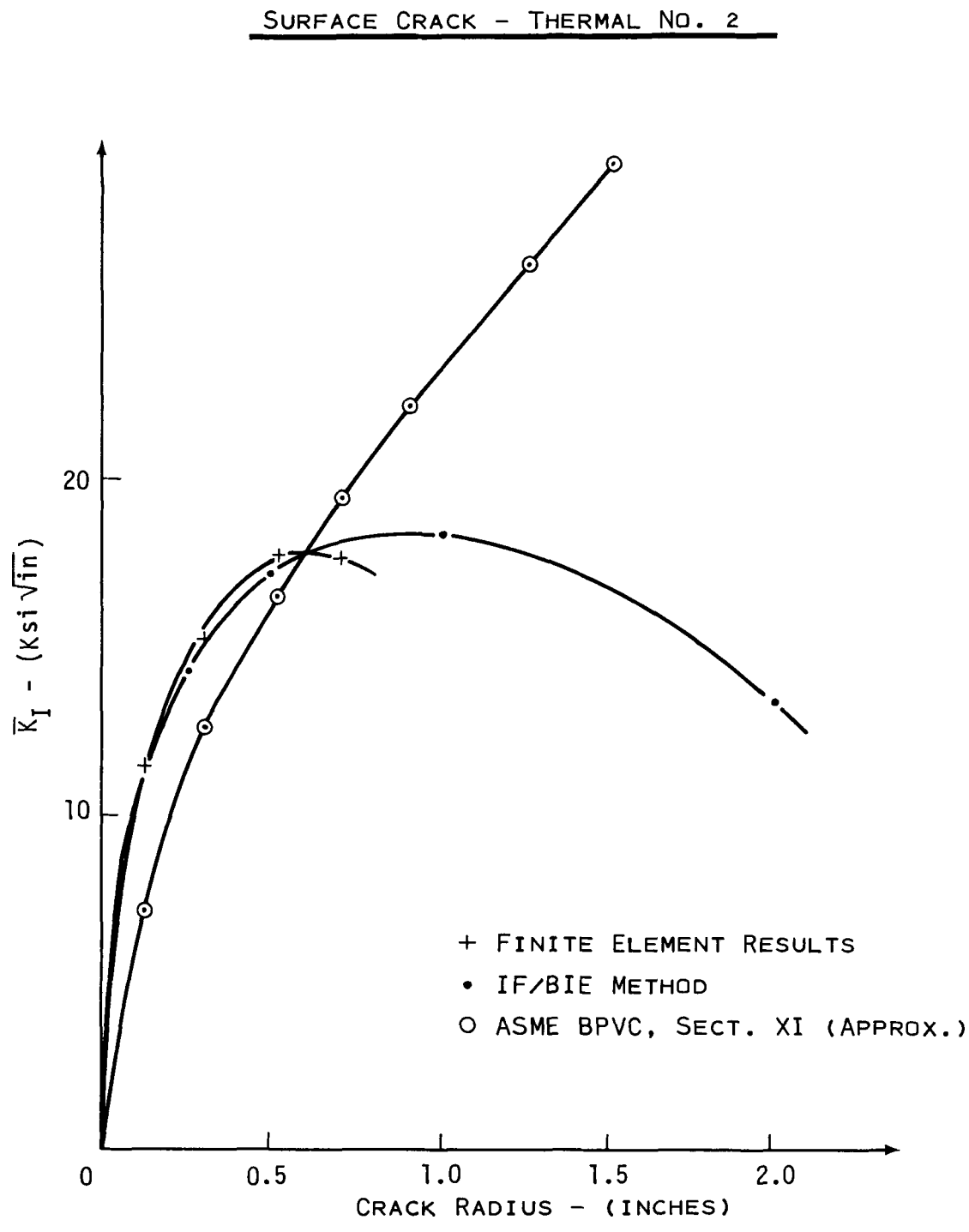

Fig. 18 - Comparison of FE, IF, and ASME Code Sector XI Methods to Compute $\bar{K}(a)$ for a Surface Crack Under Thermal Loading 2.

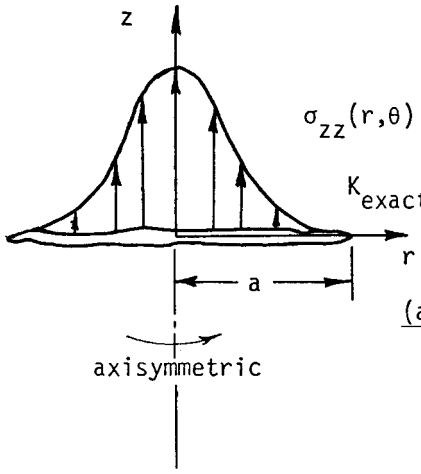

$\sigma_{zz}(r,\theta) = \sigma_{zz}(r) = (1-r^2/a^2)^5$ ksi, $r = (x^2+y^2)^{\frac{1}{2}}$

$K_{exact}(a) = \bar{K}_i(a) = K(a) = \frac{2}{11\pi}(\pi a)^{\frac{1}{2}}$ ksi $\sqrt{in}$, i = x,y

			IF Calculation		
(a in inches)	Exact K(a)	$\bar{K}_i$	Error	$\bar{K}_y$	Error
0.5	0.07253	0.0719	-0.9%	0.0718	-1.1%
1	0.10258	0.1016	-0.9%	0.1015	-1.1%
2	0.14507	0.1438	-0.9%	0.1435	-1.1%
4	0.20516	0.2033	-0.9%	0.2030	-1.1%

Penny-Shaped Crack Cross Section
(Lower Half of Stress Field Not Shown)

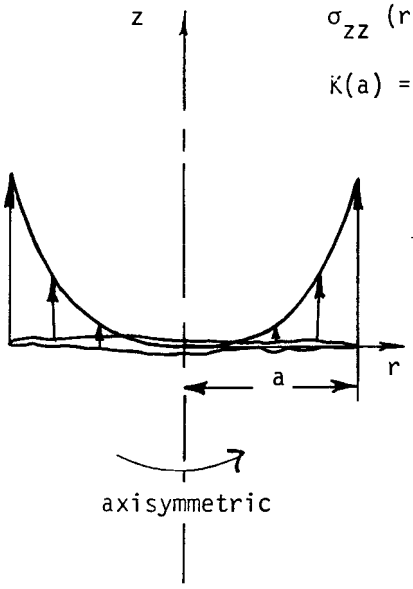

$\sigma_{zz}(r) = r^3$ ksi

$K(a) = \frac{3}{8}(\pi a^7)^{\frac{1}{2}}$ ksi $\sqrt{in}$

(a, r in inches)

			IF Calculation		
a	Exact K(a)	$\bar{K}_x$	Error	$\bar{K}_y$	Error
0.5	0.05875	0.0599	+1.9%	0.0595	+1.3%
1	0.66467	0.6774	+1.9%	0.6730	+1.3%
2	7.51988	7.6639	+1.9%	7.6141	+1.3%
4	85.07777	86.7073	+1.9%	86.1441	+1.3%

Penny-Shaped Crack Cross Section
(Lower Half of Stress Field Not Shown)

Table II. Comparison of Exact (6) and IF Method-Calculated Stress Intensity Factors for Penny-Shaped Crack in Infinite Solid Under Two Complex Symmetric Stress Fields.

model, using the strain energy release rate method. Since a three-dimensional model representing a nozzle-to-vessel intersection requires a very large number of elements, it becomes impractical to use a fine mesh to describe a crack, especially when a number of crack sizes and locations are to be considered. Therefore, a mesh has been chosen in Figs. 10a-10c which provides a reasonable balance between accuracy and computer costs. To obtain a meaningful estimate of the nozzle model accuracy, the mesh for the simplified test cases has been made similar in refinement to that of the model to be used to calculate uncracked stress in the nozzle.

The results of all five test cases (Figs. 11-13, 17, 18) indicate that the largest error has occurred for the smallest and largest crack sizes considered; the smallest because only one row of nodes and one nodal displacement was available to represent a high gradient, generally elliptical displacement shape, the largest because of an abrupt change in the element pattern near the crack tip.

In modeling the nozzle, the error for the smallest crack sizes could be lessened if elements with a higher order displacement function were used, namely, special crack tip elements or twenty-node quadratic elements. The large-crack problem would still exist for the particular case of the through-wall crack, although care could be taken to represent as smoothly as possible the area surrounding the crack.

It is believed then that the finite element method, using the strain energy release rate/stress intensity factor equivalence, would provide a reliable, though relatively expensive, technique for performing fracture mechanics analysis of a nozzle corner crack in the presence of similar thermal and mechanical loadings.

4.5 Three Additional Stress Intensity Factor Calculation Test Cases To Provide Additional Verification of the IF Method

The IF method calculates stress intensity factor estimates which are in excellent agreement with the exact solutions of Figs. 6 and 7, as shown in Table II, and in reasonable agreement with the alternating method (19) solution of the quarter-circular corner crack Test Case 8 as described in Fig. 19. These three test cases illustrate further that the IF method can compute accurately stress intensity factors for three-dimensional problems with complex stress gradients.

4.6 Summary of Comparison of Accuracy and Cost of the IF and FE Methods

Table III compares the error and cost data for the IF and FE methods for all test cases. As seen, both error and cost of fracture mechanics analyses are significantly lower for the IF method. Computer cost differences are especially large; the FE method is more than a thousand times more costly than the IF method. This is certainly not surprising, since the IF method has reduced the crack analysis problem to numerical evaluation of an area integral as described in Section 2, whereas the FE method requires a large three-dimensional numerical stress analysis. It should be noted that Table III does not include the costs necessary to generate the influence functions from three-dimensional crack analysis under simple stress fields (i.e., uniform pressure inside the crack). These costs, using the three-dimensional boundary integral equation method, have been previously mentioned in Section 2, and unlike the finite element method, are incurred only once for each crack geometry model. Table III also does not include the cost of the uncracked structural analysis.

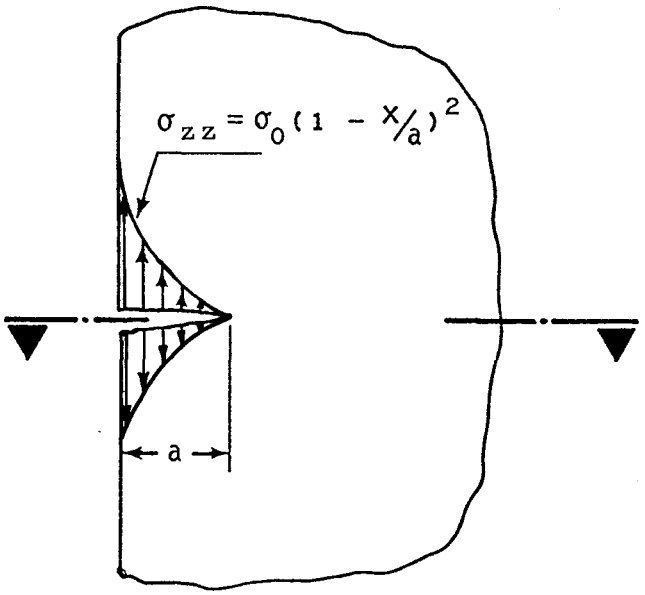

IF RESULT:

$\overline{K}_I/\sigma_0 = 0.458\sqrt{a}$

RESULT COMPUTED FROM "ALTERNATING METHOD" K(S) CALCULATION IN FIG. 3 OF (10):

$\overline{K}_I/\sigma_0 = 0.473\sqrt{a}$

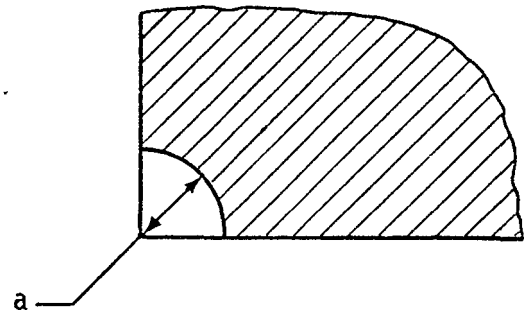

FIG. 19 - TEST CASE 9; QUARTER-CIRCLE CORNER CRACK UNDER QUADRATIC LOADING

TABLE III

COMPARISON OF ACCURACY AND COST OF THE IF AND FE METHODS FOR THREE-DIMENSIONAL ELASTIC STRESS ANALYSIS OF CRACKS

No.	Test Case Description	Percent Difference Between IF-and-FE Calculated K Values	Percent Difference Between Calculated K and Published K Values		Direct Computer Costs Required to Calculate K(a) (Dollars)		Estimated Percent Error of Best-Available Published Solution
			Influence Function	Finite Element	Influence Function	Finite Element	
1.	Circular embedded crack in an infinite solid; a uniform tensile stress field in the body, normal to the crack faces	N/A	+0.7	+2 to +8	0.6	1500	0
2.	Semicircular surface crack in a semi-infinite solid; uniform tensile stress field	N/A	+0.3 to +1.0	0 to +8	0.4	3300	±2%
3.	Quarter-circular corner crack in a quarter-infinite solid; uniform tensile stress field	N/A	-0.2 to +0.1	-3 to +4	1.0	1500	±2%
4.	Semicircular surface crack in a semi-infinite solid; complex thermal loading	-5 to +2.6	N/A	N/A	0.7	3300	N/A
5.	Additional thermal loading case	-3 to +2.7	N/A	N/A	0.7	3300	N/A
6.	Circular embedded crack in an infinite solid; a radially decreasing tensile stress distribution normal to the crack plane	N/A	-0.9	N/A	0.7	N/A	0
7.	Circular embedded crack in an infinite solid; a radially increasing tensile stress distribution normal to the crack plane	N/A	+1.9	N/A	0.7	N/A	0
8.	Quarter-circular corner crack; parabolic tensile stress normal to the crack plane	N/A	-3.1	N/A	0.9	N/A	±5%

It should also be noted that both the FE and IF results are in reasonable agreement with literature solutions (or for the thermal stress problems, with each other), and it is therefore concluded that the FE methods, as applied using the procedure in Section 3, may be successfully applied in the absence of and at greater cost than adequate IF solutions.

5.0 CONCLUSIONS

(1) Both the influence function (IF) and the finite element (FE) methods can be used to obtain accurate stress intensity factor solutions to complex thermo-mechanical three-dimensional elastic crack problems.

(2) Application of the IF method results in uniformly lower errors and more than a thousand times lower computer costs as compared to application of the FE method for three-dimensional crack analyses using available uncracked stress solutions. Therefore, the IF method is recommended for analysis of cracked structures.

(3) Appropriate and correct influence functions are not always available for implementation of the IF method. In these cases only, the FE method is recommended for obtaining stress intensity factor solutions.

(4) The Code method was never intended for and is inadequate for application to highly non-linear stress gradients and becomes excessively conservative at large values of $\underline{a}$($a > 1.0$") given the stress fields analyzed in this paper.

ACKNOWLEDGMENTS

The authors would like to acknowledge the contribution of Mr. Terry Oldberg of the Electric Power Research Institute who initially recommended that the influence function method be evaluated for possible incorporation in the subject crack analysis. We also thank Dr. Geoffrey Egan and Mr. Robert Vaile for their helpful suggestions.

REFERENCES

1. ASME Boiler and Pressure Vessel Code, Section XI, "Rules for Inservice Inspection of Nuclear Power Plant Components," 1974 edition.

2. Rashid, Y. R. and Gilman, J. D., "Three-Dimensional Analysis of Reactor Pressure Vessel Nozzles," Proceedings of the First International Conference on Structural Mechanics in Reactor Technology, G4, Berlin, Germany, 1972.

3. Besuner, P. M., "Residual Life Estimates for Structures with Partial Thickness Cracks," ASTM STP 590 (1976).

4. Besuner, P. M., "Fracture Mechanics and Residual Fatigue Life Analysis for Complex Stress Fields," FAA-EPRI-217-1-TR2 (1975).

5. Besuner, P. M., "Analysis of the Pilgrim I Nozzle-to-Pressure Vessel Weld Discontinuities," FAA-EPRI-217-1-TR6, (1975).

6. Cruse, T. A. and Besuner, P. M., "Residual Life Prediction for Surface Cracks in Complex Structural Details," AIAA Journal of Aircraft, Vol. 12, No. 4, April 1975, pp 369-375.

7. Rice, J. R., "Some Remarks on Elastic Crack-Tip Stress Fields," Int. J. Solids & Structures, Vol. 8, pp. 751-758, (1972).

8. Bueckner, H. F., "Methods of Analysis and Solutions of Crack Problems," Chapter V, Ed. by G. C. Sih, Nordhoff, (1972).

9. Besuner, P. M., "Fracture Mechanics Analysis of Rails With Shell-Initiated Transverse Defects," FAA-75-1-1(B), prepared for Association of American Railroads, November 1975.

10. "PVRC Recommendations on Toughness Requirements for Ferritic Materials,", Welding Research Council Bulletin 175, August, 1972.

11. Key, P. L., "A Relation Between Crack Surface Displacements and the Strain Energy Release Rate," Int. J. Fracture Mechanics, Vol. 5, No. 4, pp. 287-296, Noordhoff Publishing (December 1969).

12. Bergan, P. G., and Aamodt, B., Finite Element Analysis of Crack Propagation in Three-Dimensional Solids Under Cyclic Loading, in Proc. 2nd Int. Conf. Struct. Mech. in Reactor Technology, Vol. III Reactor Vessels, Berlin, September 1973.

13. FAA-DTR-76-2-02, "Influence Function Numerical Solutions for Three-Dimensional Fracture Mechanics Problems I," Report EFAA-DTR-76-2-02, 1976 (in preparation).

14. Cruse, T. A., "Application of the Boundary-Integral Equation Methods to Three-Dimensional Stress Analysis," Journal of Computers and Structures, Vol. 3, 1973, pp. 509-527.

15. Besuner, P. M. and Snow, D. W., "Application of the Two-Dimensional Integral Equation Method to Engineering Problems, "ASME, AMD, Vol. 11.

16. Snyder, M. D., and Cruse, T. A., "Boundary-Integral Equation Analysis of Cracked Anisotropic Plates," International Journal of Fracture, to be published, 1975.

17. Ricardella, P. C., "An Improved Implementation of the Boundary-Integral Technique for Two-Dimensional Elasticity Problems," Carnegie-Mellon University Report SM-72-26, September 1972.

18. Computational Fracture Mechanics, A Collection of Papers by ASME, AMD-Vol. 11, 1975.

19. Kobayashi, A., "Corner Crack at the Bore of a Rotating Disk," Submitted for ASME Publication, 1975.

20. Tada, H., Paris, P., and Irwin, G., "The Stress Analysis of Cracks Handbook," Del Research Corporation, 1973.

21. Snow, D. W., Personal Communications with P. M. Besuner, Pratt and Whitney Aircraft Division, January 1976.

22. DeSalvo, G. J., and Swanson, J. A., "ANSYS, Engineering Analysis System User's Manual," Swanson Analysis Systems, Inc., Pa., October 1972.

23. Caughey, W., Personal Communications with Swanson Analysis Systems, Inc., 1975.

24. Tracey, D. M., "Three-Dimensional Elastic Singularity Element for Evaluation of K Along an Arbitrary Crack Front," Int. J. of Frac. 9, 340-343 (September 1973).

25. Lapides, E. L. and Zebroski, E., "Use of Nuclear Plant Operating Experience to Guide Productivity Improvement Programs," EPRI Special Report SR-26-R, November 1975.

26. Cruse, T. A., "Boundary-Integral Equation Fracture Mechanics Analysis," ASME, AMD Vol. 11, 1975.

27. Cipolla, R. C., "Computerized Methods to Calculate Stress Intensity Factors Specified in ASME Code, Section XI, Appendix A," April 1975, FAA-EPRI Report #FAA-76-2-01.